

1-16-2007

# Equation of State of Looped DNA

Igor M. Kulić
*University of Pennsylvania*

Hervé Mohrbach
*Institut de Physique*

Rochish Thaokar
*Indian Institute of Technology - Bombay*

Helmut Schiessel
*Universiteit Leiden*



Suggested Citation:
I.M. Kulić, H. Mohrbach, R. Thaokar and H. Schiessel. (2007). Equation of state of looped DNA. *Physical Review E* **75**, 011913.


http://dx.doi.org/10.1103/PhysRevE.75.011913

# Equation of State of Looped DNA

**Abstract**
We derive the equation of state of DNA under tension that features a loop. Such loops occur transiently during DNA condensation in the presence of multivalent ions or permanently through sliding protein linkers such as condensin. The force-extension relation of such looped-DNA modeled as a wormlike chain is calculated via path integration in the semiclassical limit. This allows us to rigorously determine the high stretching asymptotics. Notably the functional form of the force-extension curve resembles that of straight DNA, yet with a strongly renormalized apparent persistence length. We also present analogous results for DNA under tension with several protein-induced kinks and/or loops. That means that the experimentally extracted single-molecule elasticity does not necessarily only reflect the bare DNA stiffness, but can also contain additional contributions that depend on the overall chain conformation and length.

**Disciplines**
Physical Sciences and Mathematics | Physics

**Comments**
Suggested Citation:
I.M. Kulić, H. Mohrbach, R. Thaokar and H. Schiessel. (2007). Equation of state of looped DNA. *Physical Review E* **75**, 011913.


http://dx.doi.org/10.1103/PhysRevE.75.011913

# Equation of state of looped DNA

Igor M. Kulić
*Department of Physics and Astronomy, University of Pennsylvania, Philadelphia, Pennsylvania 19104, USA*

Hervé Mohrbach
*Institut de Physique, LPMC, ICPMB (FR 2843), Université Paul Verlaine, 57078 Metz, France*

Rochish Thaokar
*Department of Chemical Engineering, Indian Institute of Technology, Bombay, Mumbai 400076, India*

Helmut Schiessel
*Instituut-Lorentz, Universiteit Leiden, Postbus 9506, 2300 RA Leiden, The Netherlands*

(Received 1 September 2005; revised manuscript received 11 October 2006; published 16 January 2007)

We derive the equation of state of DNA under tension that features a loop. Such loops occur transiently during DNA condensation in the presence of multivalent ions or permanently through sliding protein linkers such as condensin. The force-extension relation of such looped-DNA modeled as a wormlike chain is calculated via path integration in the semiclassical limit. This allows us to rigorously determine the high stretching asymptotics. Notably the functional form of the force-extension curve resembles that of straight DNA, yet with a strongly renormalized apparent persistence length. We also present analogous results for DNA under tension with several protein-induced kinks and/or loops. That means that the experimentally extracted single-molecule elasticity does not necessarily only reflect the bare DNA stiffness, but can also contain additional contributions that depend on the overall chain conformation and length.

DOI: 10.1103/PhysRevE.75.011913 PACS number(s): 87.15.La, 82.37.Rs, 05.40.−a

## I. INTRODUCTION

The DNA double helix is the molecule that encodes the genetic information in living cells. In addition to carrying the genome, DNA has also specific physical properties that are essential for its biological functions. Its mechanical properties are exploited by the protein machinery for the transcription, replication, repair, and packaging of DNA [1]. During the last decade it has been possible to manipulate single DNA molecules to determine its elastic properties under different physical conditions [2]. In these experiments, the extension of single molecule versus an applied stretching force is measured by a variety of technics, including magnetic beads [3,4], optical traps [5,6], microneedles [7], hydrodynamic flow [8], and atomic force microscopy (AFM) [9]. The studies also made it possible to better understand mechanical interactions between DNA and proteins [10].

The most appealing theoretical description of the DNA molecule is the wormlike chain (WLC) model, which is a coarse-grained model of DNA with a single parameter, the persistence length $l_p$, characterizing the chain stiffness. Originating back to the first half of the last century [11] it gained renewed interest after the semiflexible nature of DNA and other (bio)polymers became clear [12], and it is now indispensable for the theoretical understanding of many single-molecule experiments. In many cases, stiff polymers show a characteristic force-extension behavior that can be well understood in terms of the WLC as being the result of entropic fluctuations of the chain that—with increasing tension—become suppressed at shorter and shorter wavelengths. Measuring the force-extension characteristics of such a chain allows one to extracts its overall contour length as well as its persistence length.

The DNA in living cells is rarely found in its straight "naked" state; rather an overwhelming fraction of DNA is strongly configurationally constrained by binding proteins causing loops, bends, and wraps. In particular, protein complexes forming loops are essential for biological processes, such as distant gene expression or DNA packaging [1]. The formation of loops in a DNA molecule under tension has been the subject of the theoretical investigation in Ref. [13]. Also, single-molecule stretching experiments on DNA condensed with multivalent counterions performed by several groups [14,15] might bear loops or related structures, such as DNA toroids [16]. Although the statistical mechanics of unconstrained DNA under tension is well described by the WLC [12], the presence of topological constraints (such as supercoiling [17,18] and entanglements [19]) or geometrical constraints (such as protein-induced kinks and bends [20,22,21]) renders analytical results more difficult.

In this paper, we expand the repertoire of analytically solvable "equations of state" by deriving the force extension relation for a DNA with a sliding loop as depicted in Fig. 1. The computation is performed by evaluating quadratic fluctuations around the looped solution—a nonconstant saddle point of the DNA elastic energy. The method is essentially analogous to the semiclassical treatment of tunneling amplitudes in quantum mechanics [23] and instantons in quantum field theory [24]. The equation of state of looped DNA that we present here can be considered as a paradigmatic model case for stretching DNA with a nontrivial ground state. Having understood the physics of the looped DNA, it is straightforward to also extend the analysis to other cases where the overall DNA conformation is far from being straight. The calculation presented in the present work has been sketched in a previous paper [25] (for the high-force limit) together

 

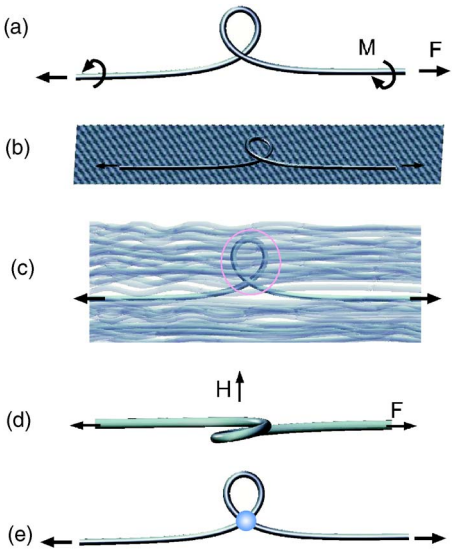


FIG. 1. (Color online) Various examples of stable loops in DNA under tension: (a) Applied torque M at the ends. (b) DNA adsorbed on a surface. (c) DNA surrounded by a dense solution of infinitely long DNAs. Unfolding of the loop goes hand in hand with an energetically costly transient "cavity" creation (in the pink gray region). (d) DNA in a strong magnetic field H perpendicular to the applied force. (e) DNA looped by a freely sliding linker ligand ("weakly condensed" DNA).

with some interesting experimental situations, namely, rigid protein-induced kinks and anchoring deflections in AFM stretching of semiflexible polymers. Expressions relating the force-extension measurements to the underlying kink and/or boundary deflection geometry were also provided in Ref. [25] and applied to the case of the GalR-loop complex [26].

The main purpose of this paper is to give a more detailed and comprehensive description of our computation presented in Ref. [25]. In addition, we also provide results by extending our method to the case of stretching DNA with many protein-induced defects (loops or kinks) and to the small force regime where the semiclassical approximation is valid only for sufficiently short DNA. Most remarkable are the results for large forces where, typically, the presence of defects modifies the elastic response of the chain in such a manner that the persistence length appears effectively reduced. For the case of DNA under tension featuring a loop, we find

$$l_P^{\mathrm{app}} = l_p\left(1 + 8\frac{l_p}{L}\right)^{-2}. \tag{1}$$

This is obviously a finite-size effect involving the scaled total length $l_p/L$, but the effect remains significant over a large range of parameters (e.g., $l_P^{\mathrm{app}} \approx 0.74 l_P$ for $L/l_p = 50$). Even for very long DNA molecules, defects (such as loops or kinks) are relevant if they are present at sufficiently high densities. Therefore, the interpretation of corresponding stretching data has to be taken with care; even though the data seem to suggest WLC behavior, the extracted value of persistence length might not reflect the real chain stiffness. Interestingly for the case of freely exchanging DNA kinking proteins and in the limit of small forces, a similar effect was recently studied analytically by Popov and Tkachenko [21].

An intriguing example that actually inspired this work is the force-extension characteristics of DNA in the presence of condensing agents such as spermidine or CoHex [14]. It shows, in some cases, a stick-release pattern, which might be attributed to the sequential unpeeling of single turns of a toroidal condensate [27]. What is important here is that in-between the force peaks one can nicely fit WLC behavior, but the persistence length that one extracts from these data is typically much lower than that of DNA. Only when the last turn is disrupted and the DNA is in a straight configuration does one find the expected value of the chain stiffness.

Before going into the theoretical analysis of looped DNA under tension, it is important to note that such a configuration is intrinsically *not* stable and therefore has to be stabilized by some mechanism. Some possible mechanisms are listed in Fig. 1(a) supercoiling in twisted DNA (the same phenomenon like in a looped telephone cable), 1(b) DNA adsorption on a surface (e.g., a liquid membrane) [28], 1(c) DNA in a dense liquid crystalline environment kinetically prohibiting the loop unfolding, 1(d) DNA in a strong magnetic field that tends to align it in a plane perpendicular to the field lines [29], and 1(e) DNA condensed by multivalent counterions as well as protein ligands that form a freely sliding link.

In Sec. II we will briefly review the Euler-Kirchhoff elastic description of the (constrained) ground states of DNA under tension. It is extremely useful for understanding the behavior of constrained "cold DNA." By "cold DNA," we metaphorically mean DNA in situations where the importance of its configurational entropy is negligible as compared to its elastic energy. This is typically the case for short DNA lengths (below its persistence length $l_P$) and large energy densities (larger than tens of $k_BT$'s per $l_P$). In Sec. II B we switch on the temperature and discuss how the thermal DNA wiggling affects its behavior. As mentioned above such "hot DNA" responds purely entropically to moderate pulling forces. We review the well-known derivation of its mechanical "equation of state," i.e., the force extension behavior of stretched DNA. In Sec. III we derive the statistical mechanics for looped DNA under tension for the most simple case where the looped DNA is confined to two dimensions as depicted in Fig. 1(b). In this context, we will learn how stretched DNA behaves when its new "ground state" is far from the straight configuration. The analytical machinery that is applied and developed further here has its roots in classical problems of physics, such as instantons in quantum-mechanical tunneling [23,24]. The unifying concept behind all these phenomena is that of path integration in the semiclassical limit. In Sec. IV, we finally calculate the stretching of looped DNA in three dimensions. We start with the case of DNA being oriented in a strong magnetic field [Fig. 1(d)]. After having given a rigorous derivation of this case, we determine the partition function for a loop stabilized by a sliding ligand [cf. Fig. 1(e)], which finally leads to Eq. (1). In Sec. V we present generalizations of our formalism (DNA with one or several kinks and/or loops) and compare our results to experiments and numerical results.

Much of the text is devoted to the development of methods and the derivation of the main results. As an inevitable

consequence not everything will be equally interesting for every reader. The readers not attracted by technical details but looking for the main physical results are advised to jump to the central results followed by browsing through the applications and discussion sections. The most interesting results are provided in Eqs. (52) and (56) (force-extension and effective persistence length for a loop in two-dimensions), Eqs. (87) and (111) and throughout Sec. V (Applications). For the reader more interested in the calculational details, we provide an overview describing the philosophy as well as possible pitfalls at the beginning of every section.

## II. PRELIMINARIES

This section mainly sets the stage and notation for the results in the following sections. In Sec. II A we review the description of DNA as an elastic beam and rederive the known force extension relation for a close to straight DNA molecule with the path integral method in Sec. II B and discuss some interesting limiting cases.

### A. Euler elastica

The basic assumption of a purely elastic description of DNA (and other semiflexible polymers as well) is that the local energy density of a given DNA state is given as a quadratic function of the underlying distortions from the straight state. Let us consider the simplest situation where the DNA twist degree of freedom can be neglected. This can be done in cases when the DNA twist is not constrained from outside, i.e., when no external torsional torques are acting on it. Then we can describe the path of the DNA of given length $L$ and bending constant $A$ subjected to an applied tension $\mathbf{F}$ by the space curve $\mathbf{r}(s)$ with the tangent $\mathbf{t}(s)=\frac{d}{ds}\mathbf{r}(s)$. It is convenient to choose the parameter $0<s<L$ as the contour length and to normalize the tangent to unity $\mathbf{t}^2(s)=1$. The elastic energy under an applied force $F$ writes in this case [30]

$$E[t]=\int_0^L \left[\frac{A}{2}\left(\frac{dt}{ds}\right)^2-\mathbf{F}\cdot\mathbf{t}\right]ds. \tag{2}$$

Here, $A$ is the bending stiffness that is usually expressed as $A=l_P k_B T$, where $l_P$ is the orientational persistence length; for DNA $l_P\approx 50$ nm [31].

Let us look first at "cold" DNA, i.e., at a molecule shorter than $l_P$ where we can, in principle, neglect entropic contributions to its behavior. The problem of finding the DNA conformation reduces in this case to the classical problem of inextensible elastic beam theory [30] of finding the energy minimizing state $\delta E/\delta \mathbf{t}=0$, which satisfies the given constraints. In a concrete computation, one would parametrize the unit tangent vector $\mathbf{t}$ in spherical coordinates $\mathbf{t}=(\cos\phi\sin\theta,\sin\phi\sin\theta,\cos\theta)$ and put the force along the $z$ axis so that the energy now writes

$$E=\int_0^L \left[\frac{A}{2}(\dot{\phi}^2\sin^2\theta+\dot{\theta}^2)-F\cos\theta\right]ds. \tag{3}$$

Note that this linear elastic ansatz can be readily extended to the description of twisted DNA states [32] by introducing another degree of freedom, the twisting angle $\psi(s)$. In this case, one has to modify Eq. (3) by adding the term $\frac{B}{2}(\dot{\phi}\cos\theta+\dot{\psi})^2$ with $B$ denoting the twist-rigidity constant that is for DNA of the same magnitude as the bending constant, $B\approx 70k_BT$ nm [31]. The reason why we can neglect it in some (but by far not all) problems is that if the twist angle $\psi$ is not explicitly constrained (no rotational torque or torsional constraining of DNA), $\psi$ can always adapt so that the $B$ multiplying term in the integral vanishes [without affecting $\phi(s)$ and $\theta(s)$].

Remarkably, as pointed out by Kirchhoff [33], the *total energy* of deformed DNA (elastic rod) can be mapped onto the *Lagrangian action* of a symmetric spinning top in a gravity field. The angles then $\theta(s)$, $\phi(s)$, and $\psi(s)$ describing the local deformations of the rod along the *contour length* $s$ become the Euler-angles $\theta(t)$, $\phi(t)$, and $\psi(t)$ of the spinning top describing the rotation of the internal coordinates system (with respect to the space fixed frame) as functions of *time* $t$. All the quantities appearing in Eq. (3) have their counterparts in the spinning top case [34]. The tension $F$ is the equivalent of the gravity force acting on the spinning top; the rigidity constants $B$ and $A$ correspond to the principal moments of inertia around the symmetry axis and perpendicular to it, respectively. The resulting rod shapes are usually called *Euler-Kirchhoff filaments* (in three dimensions) or *Euler-elastica* [in the two-dimensional (2D) case]. They are given explicitly in terms of elliptic functions and integrals [34]. The latter fact allows one, in many cases (for a given set of forces and boundary conditions), to obtain the DNA shapes in an analytical or at least numerically inexpensive manner.

### B. Semiclassical straight DNA stretching

The previous description of DNA conformations via the ground state of a purely elastic beam can, however, only be successful for very short DNA (shorter than its persistence length $l_P$). In many practical situations with the DNA molecules having lengths on the order of microns to centimeters ($\gg l_P$), one needs to go beyond the ground-state description. An important question (from the experimental and theoretical point of view) in the context of DNA stretching is the determination of the mean end-to-end distance of a DNA chain as a function of the stretching force $F$ at a finite temperature $T$ [12]. Then in order to take into account temperature effects on a WLC under tension, one has to compute the following partition function:

$$Q(\mathbf{F},L,T)=\int \delta(\underline{\mathbf{t}}^2-1)\mathcal{D}^3[\underline{\mathbf{t}}]e^{-\beta E[\underline{\mathbf{t}}]} \tag{4}$$

with the energy expression given by Eq. (2). This partition function is formally the imaginary time analytical continuation of a path integral of a quantum particle on a unit sphere subjected to an external force. The chain inextensibility constraint [represented by the $\delta$ function in Eq. (4)] makes this path integral a highly nontrivial quantity to compute as it introduces a parametrization-dependent nontrivial measure term. But, as shown below, by choosing a proper parametrization of the unit sphere, this unpleasant term does not give

any contribution if we limit the computation to the semiclassical approximation.

Let us briefly rederive the well-known results for the force-extension behavior [12]. To evaluate the path integral, we parametrize the unit vector by the Euler angles $\phi(s)$ and $\theta(s)$, i.e., $\underline{\mathbf{t}}=(\cos\phi\sin\theta,\sin\phi\sin\theta,\cos\theta)$. In this representation, the constraint in Eq. (4) is automatically satisfied and Eq. (4) becomes

$$Q(F,L,T)=\int \mathcal{D}[\phi]\mathcal{D}[\cos\theta]e^{-\beta E[\theta,\phi]}. \tag{5}$$

But as the point $\theta(s)=0$ is a singular point in spherical coordinates, we choose the force in direction parallel to the $x$ axis. This is necessary because an expansion of Eq. (3) around the straight configuration $\theta=0$ is singular and the angle $\phi(s)$ becomes arbitrary. This causes no technical problems when dealing with ground states since $\phi$ enters Eq. (3) only through its derivative $\dot{\phi}$, but we need to rotate the force direction into the $x$ direction before dealing with the statistical mechanics of hot DNA on basis of Eq. (4). It is therefore more judicious to introduce the angle $\vartheta(s)=\theta(s)-\pi/2$ such that $\underline{\mathbf{t}}=(\cos\phi\cos\vartheta,\sin\phi\cos\vartheta,-\sin\vartheta)$. Thus, the partition function writes

$$Q(F,L,T)=\int \mathcal{D}[\phi]\mathcal{D}[\vartheta]e^{-\beta E[\vartheta,\phi]-E_m[\vartheta]} \tag{6}$$

with the elastic energy

$$E[\vartheta,\phi]=\int_0^L\left[\frac{A}{2}(\dot{\phi}^2\cos^2\vartheta+\dot{\vartheta}^2)-F\cos\vartheta\cos\phi\right]ds \tag{7}$$

and with a measure expressed as

$$E_m[\vartheta]=-\delta(0)\int_0^L ds\,\log(|\cos\vartheta|), \tag{8}$$

which guarantees the $O(3)$ invariance of the measure $\mathcal{D}[\phi]\mathcal{D}[\vartheta]$ of the functional integral. The $\delta$ function at zero value of the argument should be understood as being finite using some regularization scheme (for instance, a lattice regularization, which leads to $\delta(0)\sim 1/\text{lattice constant}$, cf., e.g., [24]). Our "non-standard" parametrization of the unit vector tangential to the chain and the choice of a force pointing in the $x$ axis are necessary in order to deal properly with the measure in a semiclassical approach of the nontrivial functional Eq. (6). Instead, the standard trick for WLC is based on an analogy between the partition function and the Feynman amplitude of a quantum particle. The partition function is then approximately evaluated by determining the eigenstates of the associated quantum Hamiltonian [12,18]. This method seems to be difficult to adapt in the presence of nontrivial saddle points, even though it has been applied for tightly bent DNA [35].

Computationally, Eq. (7) with the two functions $\vartheta$ and $\phi$ entering the energy in a nonlinear manner makes the problem difficult to be treated analytically. We therefore use the harmonic approximation valid for small fluctuations around the straight configuration ($\mathbf{t}\|\mathbf{e}_x$), i.e., we expand the energy (7) at the quadratic order around the trivial saddle point ($\phi_0=\vartheta_0=0$). As $\beta$ is absent in front of the measure [Eq. (8)], this later does not participate to the selection of the saddle point, but one has to take it into account when considering quadratic fluctuations, i.e., $E_m[\vartheta]\approx-\delta(0)\int_0^L ds\,\vartheta_0^2$. The saddle point being trivial, the measure term vanishes and the partition function factorizes into two independent partition functions

$$Q(F,L,T)=e^{\beta FL}\int \mathcal{D}[\phi]e^{-(\beta/2)\int_0^L(A\dot{\phi}^2+F\phi^2)ds}\times\int \mathcal{D}[\vartheta]e^{-(\beta/2)\int_0^L(A\dot{\vartheta}^2+F\vartheta^2)ds}. \tag{9}$$

so that, we only have to compute

$$Q_1(F,L,T)=\int \mathcal{D}[\phi]e^{-(\beta/2)\int_0^L(A\dot{\phi}^2+F\phi^2)ds}. \tag{10}$$

Note that this factorization property and, in particular, the cancellation of the measure are due to our choice of the coordinate system.

In order to later compare the free energy of the straight chain with that of the looped configuration, we compute the path integral with the boundary conditions $\phi(0)=\vartheta(0)=0$ and $\phi(L)=\vartheta(L)=0$, which are the most convenient choice for a semiclassical evaluation of the path integral around a nontrivial saddle point. The Fourier decomposition is then restricted to sine functions $\phi(s)=\Sigma\sqrt{2/L}\sin(\omega_m s)\phi_m$ with frequencies $\omega_m=\pi m/L$. The evaluation of the path integral then reduces to the computation of a product of Gaussian integrals leading to

$$Q(F,L,T)=\frac{\beta\sqrt{AF}}{2\pi}\frac{e^{\beta FL}}{\sinh\left(L\sqrt{\frac{F}{A}}\right)}. \tag{11}$$

The force-extension relation can then be deduced from the expression $\langle\Delta x\rangle=-\partial G/\partial F$, where $G(F,L,T)=-\frac{1}{\beta}\ln Q(F,L,T)$ is the free energy of the system. We then obtain

$$\frac{\langle\Delta x\rangle}{L}=1+\frac{1}{2\beta FL}-\frac{1}{2\beta\sqrt{FA}}\coth\left(\frac{L}{\lambda}\right). \tag{12}$$

Here we introduced the quantity $\lambda=\sqrt{A/F}$, usually called the *deflection length* or *tension length* [20,36], which becomes the relevant length scale in the case of DNA under tension replacing the usual (tension-free) persistence length $l_P=A/k_BT$.

From the force-extension relation [Eq. (12)], we see that two limiting cases corresponding to regimes of small forces $L/\lambda\ll 1$ and large forces $L/\lambda\gg 1$ can be studied analytically.

#### *1. Small forces regime: $L/\lambda\ll 1$*

One can readily see that this condition implies a small force regime $\beta FL\ll l_p/L$, which is compatible with the harmonic approximation only if the persistence length is much larger than the chain length ($l_p\gg L$). Then in this case, Eq. (12) becomes

$$\frac{\langle \Delta x \rangle}{L} \approx 1 - \frac{L}{6l_p} + \frac{L^3}{24 l_p} \frac{F}{A} \approx 1 - \frac{L}{6l_p}, \tag{13}$$

i.e., thermal fluctuations lead in leading order to a force-independent small reduction of the end-to-end distance.

#### 2. Large forces regime: $L/\lambda \gg 1$

This regime implies the condition $\beta F L \gg l_p/L$, which can be made compatible with the harmonic approximation for any value of the ratio $l_p/L$. The free energy of the WLC under tension is then approximately given by

$$G(F,L,T) \approx -FL + \frac{L}{\beta}\sqrt{\frac{F}{A}} - \frac{1}{\beta}\ln\left(\frac{\beta\sqrt{AF}}{2\pi}\right), \tag{14}$$

whereas the force-extension relation in this limit becomes

$$\frac{\langle \Delta x \rangle}{L} \approx 1 - \frac{1}{2\beta\sqrt{FA}} + \frac{1}{2\beta FL}. \tag{15}$$

In this force regime, the term $O(1/\beta FL)$ can always be neglected and one arrives at the important formula [12]

$$\frac{\langle \Delta x \rangle}{L} \approx 1 - \frac{k_B T}{2\sqrt{AF}}. \tag{16}$$

This can be solved for the force

$$F \approx \frac{k_B T}{4 l_P} \frac{1}{(1 - \langle \Delta x \rangle / L)^2}. \tag{17}$$

The force [Eq. (17)] is of entropic origin as the proportionality to temperature indicates. Equation (17) turned out to be a very powerful tool for directly and accurately determining the persistence length of DNA molecules from micromanipulation experiments under a multitude of conditions [2]. One should note that Eq. (17) is only valid in the limit of large forces $\left(F \gg \frac{k_B T}{4 l_P} = 20 \text{ fN}\right)$ and large relative extensions $\langle \Delta z \rangle / L \approx O(1)$. Looking at its simplicity, it is somehow surprising that it is experimentally accurate for piconewton forces almost up to the point where DNA starts to melt and the WLC description breaks down (~60 pN).

To have an expression that also includes very low forces (on the femtonewton scale), one usually uses the following interpolation formula [12]:

$$F = \frac{k_B T}{l_P}\left[\frac{1}{4\left(1 - \frac{\langle \Delta z \rangle}{L}\right)^2} - \frac{1}{4} + \frac{\langle \Delta z \rangle}{L}\right]. \tag{18}$$

In the limit of small extensions, $\langle \Delta z \rangle / L \ll 1$, one recovers $F = \frac{3}{2}\frac{k_B T \langle \Delta z \rangle}{l_P L}$, which is the force that one expects for a Gaussian coil perturbed by weak forces [37]. For large forces, one asymptotically recovers Eq. (17).

## III. THE LOOP IN TWO DIMENSIONS

In the following, we consider a DNA chain under tension that contains a sliding loop. The corresponding shape at zero temperature is that of the homoclinic loop [38] that is a solution of the Euler-Lagrange equations. This filament shape, which was already considered by Euler [34], is two-dimensional. For any given finite tension $F$, the homoclinic loop turns out to be stable for arbitrarily large *in-plane* perturbations. Indeed, the 2D homoclinic loop can be considered as a (static) topological soliton appearing in many contexts of contemporary physics, ranging from Josephson-junctions, dislocations in solids [39] to QM tunneling problems [23,24]. In this section, we study the DNA chain being confined to two dimensions and, in Sec. IV, we go into the third dimension by allowing also out-of-plane fluctuations.

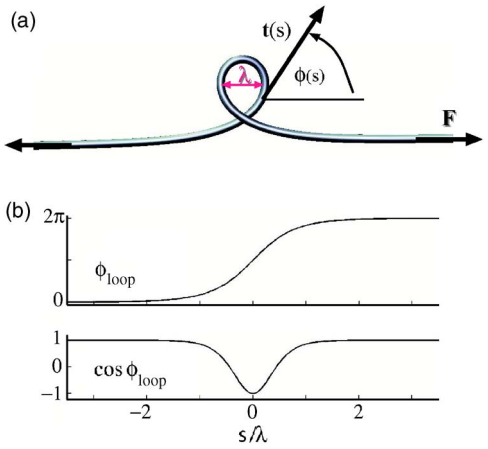


FIG. 2. (Color online) (a) The definition of the Euler angle $\phi$ and the scale of the loop. The loop head diameter [red (dark gray)] is approximately given by $\lambda = \sqrt{A/F}$. (b) The loop solution $\phi_{\text{loop}}(s)$ as given by Eq. (46).

In Sec. III A, we derive the partition function for 2D loop under tension. The only technical difficulty—the presence of a close-to-zero (translational) mode [cf. Fig. 3(a)]—is dealt with in close analogy to instanton tunneling [23]. In Sec. III B, we provide the corresponding force-extension relation with a special focus on limiting cases. In the most important limit of large forces, we provide the main results of this section [Eqs. (52) and (56)]. These equations demonstrate an effective length-dependent renormalization of the apparent persistence length induced by the presence of a trapped loop.

### A. Partition function

Consider a looped DNA chain under tension $F$ along the $x$ axis. In this section, the DNA is only allowed to fluctuate in-plane [as it is the case for a chain adsorbed on a fluid membrane, cf. Fig. 1(b)]. We neglect the DNA twist degree of freedom that, in general, if not explicitly constrained, decouples from the DNA bending energy. To obtain the force-extension behavior of the loop in two dimensions, we semiclassically evaluate the partition function $Q_{\text{loop}}$ by considering quadratic fluctuations around the saddle point $\phi_{\text{loop}}$ that is, here, the loop configuration. We impose that the angles at the extremities of DNA are clamped in an orientation parallel to the force direction, so that $\phi(-L/2)=0$ and $\phi(L/2)=2\pi$, where $\phi$ denotes the angle between the tangent vector $\underline{\mathbf{t}}=(\cos\phi, \sin\phi)$ and the $x$ axis [cf. Fig. 2(a)]. Then

the partition function in two dimensions corresponds to the following quantum probability amplitude expressed in terms of a path integral:

$$Q_{\text{loop}} = \left\langle 0, \frac{-L}{2\lambda} \middle| 2\pi, \frac{L}{2\lambda} \right\rangle = \int_{(0,-L/2\lambda)}^{(2\pi,L/2\lambda)} \mathcal{D}[\phi] e^{-\beta E[\phi]}. \tag{19}$$

The DNA energy $E[\phi]$, which is the 2D analog of Eq. (7) can be written

$$E[\phi] = \sqrt{AF} \int_{-L/2\lambda}^{L/2\lambda} \left( \frac{1}{2}\dot{\phi}^2 - \cos\phi \right) dt \tag{20}$$

with the dimensionless contour length $t=s/\lambda$; dots represent, from now on, derivatives with respect to $t$. Note that the nontrivial measure term [Eq. (8)] is absent in the 2D case. In the spirit of the Kirchhoff kinetic analogy from Sec. II A, the bending energy in Eq. (20) corresponds to the Lagrangian of a spherical pendulum in the gravitational field. We now expand $E[\phi]$ up to quadratic order around the minimum configuration $\phi_{\text{loop}}$ by introducing a fluctuating field $\delta\phi$ such that $\phi=\phi_{\text{loop}}+\delta\phi$. The linear term $\delta E$ in this expansion vanishes because $\phi_{\text{loop}}$ is an extremum point of $E$, and we have

$$E[\phi_{\text{loop}} + \delta\phi] = E_{\text{loop}} + \delta^2 E[\phi_{\text{loop}}]. \tag{21}$$

#### 1. Saddle-point contribution

To determine the saddle-point configuration, we solve the Euler-Lagrange equations of Eq. (20) that gives the following nonlinear equation:

$$\ddot{\phi} = \sin\phi. \tag{22}$$

Besides the trivial solution $\phi=0$ that corresponds to the ground state but cannot describe a loop configuration, there exist other topological solutions of Eq. (22) that are appropriately called solitons or kinks. Now Eq. (22) can be integrated twice to obtain

$$(t - t_0) = \int_{\phi(t_0)}^{\phi(t)} \frac{d\phi'}{\sqrt{2(C - \cos\phi')}} \tag{23}$$

with an integration constant $C$. The general solution of Eq. (22) with arbitrary $C$ leads to elliptic functions. With the condition $t_0=0$ and $\phi(0)=\pi$ the solution reads

$$\cos\phi_{\text{loop}}(t) = 2\,\text{sn}^2\left( \frac{t}{\sqrt{m}} \middle| m \right) - 1 \tag{24}$$

$$\phi_{\text{loop}}(t) = \pi + 2\,\text{am}\left( \frac{t}{\sqrt{m}} \middle| m \right) \tag{25}$$

with "sn" and "am" being the Jacobian elliptic function with parameter $m$ [40] whose value is related to $C$ in Eq. (23) via $m=2/(1+C)$. The parameter $m$ with the range $0 \leqslant m \leqslant 1$ results from the clamped boundary conditions and is implicitly given by

$$\sqrt{m}K(m) = \frac{L}{2\lambda} = \frac{L}{2}\sqrt{\frac{F}{A}} \tag{26}$$

with $K(m)$ denoting the complete elliptic integral of the first kind [40]. In the Kirchhoff analogy, the solution [Eq. (24)] describes a revolving pendulum that makes one full turn during the "time period" $L/\lambda$.

The "classical" ($T=0$) bending energy of the loop as an implicit function of the force is then given by

$$\beta E[\phi_{\text{loop}}] = 4\frac{l_P}{L}K(m)[K(m)(m-2) + 4E(m)], \tag{27}$$

where $E(m)$ is the complete elliptic integral of the second kind [40]. We now compute the contribution of the quadratic fluctuations around this looped saddle point to the partition function.

#### 2. Fluctuation contributions

In the semiclassical approximation (see, for instance, [23], Chap. 4), the partition function [Eq. (19)] can be written as a product of an energetic contribution and a quadratic path integral over the fluctuating fields $\delta\phi$ satisfying the Dirichlet boundary conditions $\delta\phi(-\frac{L}{2\lambda})=\delta\phi(+\frac{L}{2\lambda})=0$

$$Q_{\text{loop}} = e^{-\beta E_{\text{loop}}} Q_{\text{loop}}^{\text{fluct}} \tag{28}$$

with the partition function corresponding to the quadratic fluctuation contributions given by

$$Q_{\text{loop}}^{\text{fluct}} = \int \mathcal{D}[\delta\phi] e^{-(\beta\sqrt{AF}/2)\int_{-L/2\lambda}^{L/2\lambda} \delta\phi \hat{\mathbf{T}} \delta\phi dt} = \sqrt{\frac{\beta\sqrt{AF}}{2\pi D\left(-\frac{L}{2\lambda}, \frac{L}{2\lambda}\right)}}. \tag{29}$$

Here, $D(-\frac{L}{2\lambda}, \frac{L}{2\lambda})$ is the determinant associated with the quadratic fluctuation operator $\hat{\mathbf{T}}$ that reads

$$\hat{\mathbf{T}} = \left[ -\frac{\partial^2}{\partial t^2} + 2\,\text{sn}^2\left( \frac{t}{\sqrt{m}} \middle| m \right) - 1 \right]. \tag{30}$$

The problem of finding the eigenvalues (EV) of this operator falls into a class of "quasi exactly solvable" problems and typically appears in quantum mechanical problems. The corresponding differential equation is called the Lamé equation [41]. It admits simple solutions in terms of polynomials of elliptic functions sn, cn, and dn. Its discrete spectrum is known [41] and writes

$$\phi_{-1}(t) = \text{cn}\left( \frac{t}{\sqrt{m}} \middle| m \right) \quad \text{with EV } \frac{1}{m} - 1,$$

$$\phi_0(t) = \text{dn}\left( \frac{t}{\sqrt{m}} \middle| m \right) \quad \text{with EV } 0,$$

$$\phi_1(t) = \mathrm{sn}\left(\frac{t}{\sqrt{m}}|m\right) \quad \text{with EV } \nu_1 = \frac{1}{m}. \tag{31}$$

One sees immediately that the only eigenfunction satisfying the Dirichlet boundary condition is $\phi_{-1}$ and the corresponding smallest EV of $\hat{\mathbf{T}}$ we denote in the following by

$$\mu_0 = \frac{1-m}{m}. \tag{32}$$

Therefore for a molecule of finite length, there is no zero mode, but $\mu_0$ goes to zero in the limit of infinite length $L$ that, in terms of $m$, corresponds to the limit $m \to 1$. The existence of a vanishing eigenvalue is the consequence of the translational invariance $t \to t+t_0$ of the loop solution that formally causes a divergence of Eq. (29) (see [23], Chap. 17, or [24], Chap. 36).

The determinant $D\left(-\frac{L}{2\lambda}, \frac{L}{2\lambda}\right)$ can be computed directly via the method of Gelfand and Yaglom [42] that consists of solving an initial value problem on the interval $[-L/2\lambda, L/2\lambda]$. The explicit solution for $D\left(\frac{L}{2\lambda}, -\frac{L}{2\lambda}\right)$ can be stated in terms of the classical solution $\phi_{\mathrm{loop}}(t)$

$$D\left(-\frac{L}{2\lambda}, \frac{L}{2\lambda}\right) = \dot{\phi}_{\mathrm{loop}}\left(\frac{L}{2\lambda}\right)\dot{\phi}_{\mathrm{loop}}\left(-\frac{L}{2\lambda}\right)\int_{-L/2\lambda}^{L/2\lambda} \frac{dt}{[\dot{\phi}_{\mathrm{loop}}(t)]^2} = 2\sqrt{m}E(m). \tag{33}$$

This expression, however, has to be taken with caution since it is incorrect for large values of $L/\lambda$ missing a factor $\sim e^{-\frac{L}{2}\sqrt{\frac{F}{A}}}$, which corresponds to the fluctuation contribution of the linear part of the DNA. To solve this problem, one has to take the approximate translational invariance of the loop in the limit $m \to 1$ into account. The way to deal rigorously with a zero mode in the infinite $L$ case is well known (see [23], Chap. 17, or [24], Chap. 36): One has to consider an infinite number of degenerate saddle points resulting from the translational invariance.

To do this, we first expand $\delta\phi(t)$ in a complete set of orthonormal eigenvectors $\phi_n(t)$ diagonalizing the operator $\hat{\mathbf{T}}$, i.e., $\delta\phi(t) = \Sigma_{n=0}^{\infty} a_n \phi_n(t)$. Next we consider the "collective position coordinate" $t_0$ (defining the central position of the loop on the chain) as an integration variable in the path integral. $t_0$ is related to (but not identical with) normal mode $a_0$ associated with the zero mode eigenfunction $\phi_0(t)$ and can be expressed as $t_0(a_0) = J(m)a_0$ with a Jacobian $J(m) = \partial t_0 / \partial a_0$ determined below. For a finite chain length, the loop center will be approximately confined to a finite interval between the two DNA ends (i.e., we have $-L/2\lambda < t_0 < L/2\lambda$). Taking this into account, a corrected determinant $D_{\mathrm{corr}}$ can be computed by removing the would-be-zero mode from the determinant and by reinserting explicitly the actual (finite interval) contribution of the same mode

$$\left[D_{\mathrm{corr}}\left(-\frac{L}{2\lambda}, \frac{L}{2\lambda}\right)\right]^{1/2} = \frac{\int_{-\infty}^{\infty} e^{-(\beta\sqrt{AF}/2)\mu_0 a_0^2} da_0}{\int_{-\alpha}^{\alpha} e^{-(\beta\sqrt{AF}/2)\mu_0 a_0^2} da_0}\left[D\left(-\frac{L}{2\lambda}, \frac{L}{2\lambda}\right)\right]^{1/2}. \tag{34}$$

The integration boundaries $\pm\alpha$ of the $a_0$ integral in the denominator are related to the Jacobian via $\pm L/2\lambda = \pm(\partial t_0/\partial a_0)\alpha$. To determine $\partial t_0/\partial a_0$ consider a small translation of the loop $\partial\phi_{\mathrm{loop}}$. On the one hand we have simply $\partial\phi_{\mathrm{loop}} = \dot{\phi}_{\mathrm{loop}}\partial t_0$. On the other hand the same translation can be performed by the action of the eigenfunction $\phi_0(t)$ and we obviously have $\partial\phi_{\mathrm{loop}} = \phi_0 \partial a_0$. Combining these two expressions for $\partial\phi_{\mathrm{loop}}$, we obtain $\partial t_0/\partial a_0 = \phi_0/\dot{\phi}_{\mathrm{loop}} = \left(\frac{\sqrt{m}}{8E(m)}\right)^{1/2}$ and we deduce $\alpha = \frac{L}{2\lambda}\left(\frac{8E(m)}{\sqrt{m}}\right)^{1/2}$. Inserting this into Eq. (34), the corrected partition function finally reads

$$Q_{\mathrm{loop}} = \left(\frac{\beta\sqrt{AF}}{4\pi\sqrt{m}E(m)}\right)^{1/2} \mathrm{erf}\left(\sqrt{\frac{\beta\sqrt{AF}\mu_0 E(m)}{\sqrt{m}}}\frac{L}{\lambda}\right) \times e^{-2(\beta\sqrt{AF}/\sqrt{m})[K(m)(m-2)+4E(m)]}. \tag{35}$$

Using the relations (26) and (32), we can rewrite this expression fully in terms of $m$,

$$Q_{\mathrm{loop}}(m) = \left(\frac{l_P}{2\pi L}\frac{K(m)}{E(m)}\right)^{1/2} \mathrm{erf}\left[2\left(2\frac{l_P}{L}\right)^{1/2} K^{3/2}(m)E^{1/2}(m) \times (1-m)^{1/2}\right] e^{-4(l_P/L)K(m)[K(m)(m-2)+4E(m)]}. \tag{36}$$

Note that the erf function (coming from the close to zero-mode contribution) only differs significantly from unity for values of $m \approx 1$, which corresponds to the long DNA limit $L/\lambda \gg 1$. This is consistent with our intuition as only in the long-chain limit the loop can move freely. The constraint equation (26) can be solved for $m \approx 1$ giving $m \approx 1 - 16e^{-(L/\lambda)}$, showing that the smallest eigenvalue $\mu_0$ [Eq. (32)] reads $\mu_0 = 16e^{-(L/\lambda)}$. Thus, indeed, as intuitively expected, this eigenvalue becomes asymptotically zero for $L/\lambda \to \infty$ (i.e., $m \to 1$).

### B. Force-Extension Relation

The force-extension relation of the looped chain in two dimensions follows from the free energy $G_{\mathrm{loop}} = -\beta^{-1}\ln(Q_{\mathrm{loop}})$ via $\langle\Delta x\rangle = -\partial G_{\mathrm{loop}}/\partial F$ with $Q_{\mathrm{loop}}$ given by Eq. (36). Because of the structure of $Q_{\mathrm{loop}}$, the mean extension is a sum of three terms: a contribution from the bending energy $\Delta_E x$, a second one from fluctuations around the loop configuration $\Delta_{\|} x$, and a third from the zero-mode correction $\Delta_{\mathrm{err}} x$, i.e.,

$$\langle\Delta x\rangle = \langle\Delta_E x\rangle + \langle\Delta_{\|} x\rangle + \langle\Delta_{\mathrm{err}} x\rangle. \tag{37}$$

The saddle-point contribution to the mean extension is given by

$$\langle \Delta_E x \rangle = \frac{L}{m}\left[\frac{(2-m)K(m)-2E(m)}{K(m)}\right]. \tag{38}$$

The contribution resulting from fluctuations around the loop configuration is given by

$$\langle \Delta_{\|} x \rangle = \frac{L^2}{16 l_p m}\left[\frac{E^2(m)+(1-m)K^2(m)-2(1-m)E(m)K(m)}{[E(m)K(m)]^2}\right]. \tag{39}$$

Finally, the contribution coming from the error function (zero-mode correction) is

$$\langle \Delta_{\mathrm{err}} x \rangle = \frac{L(1-m)[3E^2(m)-(1-m)K^2(m)-2E(m)K(m)]}{2\sqrt{2\pi}m\ \mathrm{erf}\left[2\left(2\frac{l_P}{L}\right)^{1/2}K^{3/2}(m)E^{1/2}(m)(1-m)^{1/2}\right]} \times \frac{e^{-(8l_p/L)(1-m)E(m)K^3(m)}}{E(m)\sqrt{\frac{l_p}{L}(1-m)E(m)K(m)}}. \tag{40}$$

This allows one to immediately plot force-extension curves for a loop in two dimensions. We dispense here with giving such a plot since the curves turn out to be very similar to the corresponding ones in three dimensions (presented later in Fig. 4). Instead, we only extract from Eqs. (38)–(40) the limiting cases of small and large forces.

#### 1. Limit of small values of $m \approx 0$

This corresponds to a regime of small forces $L/2\lambda \ll 1$, valid only for chains satisfying $l_p/L \gg 1$. In this limit, the functions $\mathrm{sn}(x|\mathrm{m}) \sim \sin(x)$ and $\mathrm{am}(x|\mathrm{m}) \sim x$, so that the loop configuration given by Eq. (24) corresponds to a circle $\phi_{\mathrm{loop}}(s) = \pi + 2s\pi/L + O(m)$. The bending energy is then given by

$$\beta E_{\mathrm{circle}} = 2\pi^2 \frac{l_P}{L} + O(m), \tag{41}$$

where we used $K(m)$, $E(m) \approx \pi/2 + O(m)$ for $m$ very small.

To determine the force-extension relation, we expand the various contributions in expression (38) to the first order in $m$ and replace $m$ by $\frac{L^2}{\pi^2}\frac{F}{A}$. We then arrive at

$$\langle \Delta_E x \rangle \approx \frac{L}{8\pi^2 l_p}\frac{FL^2}{k_B T} + O(m^2), \tag{42}$$

which shows that the bending energy contribution to the elongation goes to zero with the force. This is expected as the bending energy is independent of the force when $m$ goes to zero by virtue of Eq. (41). In the same manner, we obtain the contribution due to the quadratic fluctuations around the loop

$$\langle \Delta_{\|} x \rangle \approx \frac{L^2}{4\pi^2 l_p} + O(m^2). \tag{43}$$

We find here that the thermal fluctuations cause on average an increase of the end-to-end distance (resulting in a reduction of the loop size). Note that this is contrary to the stretching of a linear DNA, where entropic effects lead to a shortening of the polymer [cf. Eq. (13)].

As the loop cannot slide in this context, the contribution of the close to zero-mode correction to the force-extension relation should vanish. Indeed, our computation gives

$$\langle \Delta_{\mathrm{err}} x \rangle \approx -\frac{120}{\pi^2}\frac{L^2}{l_p} e^{-(\pi^4 l_p/2L)}[1 + O(m^2)], \tag{44}$$

which is negligible due to $l_p/L \gg 1$.

In conclusion in the regime $\frac{L}{2\lambda} \ll 1$, the force extension relation is given by

$$\frac{\langle \Delta x \rangle}{L} \approx \frac{L}{4\pi^2 l_p}\left(1 + \frac{\beta F L}{2}\right), \tag{45}$$

i.e., for short, almost circular, looped chains the extension grows linearly with the force.

#### 2. Limit $m \approx 1$: The homoclinic loop case

In the limit $m \to 1$, $K(m)$ diverges as $\ln(4/\sqrt{1-m})$ and $E(m) \approx 1$. By virtue of Eq. (26), this corresponds then to the case $L/2\lambda \gg 1$ (strong force regime), where the length of the molecule is very large compared to the loop size of order $\lambda$. In this case, expression (25) reduces to a "kink" configuration $\phi_{\mathrm{loop}} = 4 \arctan e^t$ with $\phi(-\infty) = 0$ and $\phi(+\infty) = 2\pi$ (cf. also Fig. 2). Equation (24) is then given by

$$\cos \phi_{\mathrm{loop}}(t) = 1 - \frac{2}{\cosh^2(t)}. \tag{46}$$

This saddle-point solution is correct only in the infinite chain limit, but for finite large length the corrections are of order $e^{-L/\lambda}$. This implies that the bending energy of the kink is then given by

$$E_{\mathrm{loop}} = E[\phi_{\mathrm{loop}}] = -FL + 8\sqrt{AF} + O(e^{-L/\lambda}). \tag{47}$$

The fluctuating quadratic operator in this long-chain limit is

$$\hat{\mathbf{T}} = \left[-\frac{\partial^2}{\partial t^2} + \left(1 - \frac{2}{\cosh^2(t)}\right)\right]. \tag{48}$$

It is interesting to note that this operator is identical to the fluctuation operator of a kink or instanton solution [Eq. (46)] that appears in the semiclassical treatment of a quantum particle tunneling in a double-well potential (cf. [23,24]). Using this analogy, one can independently derive all the results given here in the $m \to 1$ limit as done in [25].

With the more general expression [Eq. (36)] at hand, we can directly take the limit $m \to 1$, which leads to the partition function

$$Q_{\mathrm{loop}} \approx \frac{4}{\pi}\beta L F e^{-(L/2)\sqrt{F/A}} e^{-\beta(8\sqrt{FA} - LF)} \tag{49}$$

from which we deduce the free energy

$$G_{\mathrm{loop}} \approx \frac{L}{2\beta}\sqrt{\frac{F}{A}} + 8\sqrt{AF} - LF - \frac{1}{\beta}\ln\left(\frac{4}{\pi}\beta L F\right). \tag{50}$$

We now compare this free energy to that of the straight state. Note that we cannot use Eq. (14) because it corre-

sponds to 3D case. Instead, we need the 2D free energy, which derives from a partition function, that is evidently given by $Q(F,L,T)=e^{\beta FL}Q_1(F,L,T)$. This means that the second and third terms of the free-energy expression [Eq. (14)] have to be divided by 2. Subtracting that free energy, $G_0$, from $G_{\mathrm{loop}}$ leads to the free-energy difference

$$\Delta G_{\mathrm{loop-0}} = G_{\mathrm{loop}} - G_0 = 8\sqrt{AF} + O\left[\frac{1}{\beta}\ln\left(\frac{LF}{k_BT}\frac{l_P}{\lambda}\right)\right]. \tag{51}$$

Then we see that the free-energy difference $\Delta G_{\mathrm{loop-0}}$ is dominated by the elastic energy part $8\sqrt{AF}$, which is the second term in $E_{\mathrm{loop}}$ [Eq. (47)]. The first term $-FL$ is already present in the straight DNA case and cancels in the difference. Besides that (typically very large) term, there is merely a logarithmic correction. We note that a weak coupling of the thermal fluctuations to a DNA shape has also been observed by Odijk [35] for circular DNA rings.

The force-extension curve of a 2D loop is then calculated via $\langle \Delta x\rangle = -\partial G_{\mathrm{loop}}/\partial F$

$$\frac{\langle \Delta x\rangle}{L} = 1 - \left(\frac{1}{4} + 4\frac{l_P}{L}\right)\frac{1}{\beta\sqrt{AF}} + \frac{1}{\beta FL}. \tag{52}$$

To understand the origin of each of the various contributions to Eq. (52), we now consider the limit $m \to 1$ of Eq. (37). We find for the energetic contribution

$$\langle \Delta_{\mathrm{E}} x\rangle \underset{m\to 1}{\approx} L\left(1 - \frac{4}{L}\sqrt{\frac{A}{F}}\right). \tag{53}$$

The sum of the two other purely entropic contributions (including the zero-mode correction) is given by

$$\langle \Delta_{\parallel} x\rangle + \langle \Delta_{\mathrm{err}} x\rangle \underset{m\to 1}{\approx} \frac{-L}{4\beta\sqrt{AF}} + \frac{1}{\beta F}. \tag{54}$$

The first term in Eq. (54) corresponds to the fluctuation of the linear part (in two dimensions) of the DNA [compare to the corresponding 3D term in Eq. (15)], whereas the second term is negligible. Combining the different contributions we recover Eq. (52). We may drop the last contribution $1/\beta FL$, which is for all practical purposes negligible.

We can now compare the equation of state of the looped DNA [Eq. (52)] to the one for the straight configuration in two dimensions given by $\langle \Delta x_0\rangle = -\partial G_0/\partial F$

$$\frac{\langle \Delta x_0\rangle}{L} = 1 - \frac{1}{4}\frac{1}{\sqrt{\beta F l_P}}. \tag{55}$$

Comparing Eqs. (52) and (55), we see that both have a leading term proportional to $F^{-1/2}$; only the prefactor in Eq. (52) is renormalized by a contribution stemming from the elastic part of the loop free energy.

This implies a fairly simple prediction that is useful for the interpretation of experimental data: Suppose one performs a single-molecule stretching experiment with a DNA chain that contains a loop. If one does not know about the presence of the loop, one will fit the data by the usual WLC expression [Eq. (55)] and is happy that it works well (at least up to the leading term $F^{-1/2}$). From that fit, the total length of the DNA is recovered correctly (from the asymptotic line on the $\Delta x$ axis), but something strange seems to have happened to the "persistence length"—it is smaller than expected. The explanation is simple: The *apparent persistence length* becomes

$$l_P^{\mathrm{app}} = \frac{l_P}{\left(1 + 16\frac{l_P}{L}\right)^2} \text{ in two dimensions.} \tag{56}$$

This formula is similar to Eq. (1), with a factor 16 instead of 8 in front of the $l_P/L$ term. The difference comes from the fact that we allow, here, only fluctuations in two dimensions. The 3D case will be studied in Sec. IV.

## IV. HOMOCLINIC LOOP IN THREE DIMENSIONS

After having understood the behavior of the homoclinic loop in two dimensions, it seems that a generalization to the third dimension should be straightforward. But as we will see, there are several traps and some interesting physics on the way. The first and main problem is the fact that the homoclinic loop is, unlike in the 2D case, elastically unstable (in sharp contrast to a false claim in literature [43]), and one has to introduce forces or constraints necessary for its stabilization. A simple way to see this is to take an elastic cable, make a loop in it, and pull on it (without torsionally constraining the ends). Only if we force the loop to stay in a plane (for instance, its own weight can perform this task if the cable is lying on a table provided that we do not pull too strongly), it represents a *topological excitation* that cannot leave the rod (except at either of its two ends). Thus, if there is any interesting physics of 3D homoclinic loops, it will have to come through constraints or loop-stabilizing potentials. In the following, we mainly consider two stabilizing procedures: In one case, we carefully remove the unstable mode from the partition function (the loop is then approximately forced to stay in a plane) and, in the second case, we evaluate the partition function in the presence of an explicit self-interaction that stabilizes the loop. It is then shown that for very long chains the fashion via which the loop is stabilized is irrelevant with regard to the determination of the force-extension relation.

In Sec. IV A, we deal with the presence of two normal modes of the chain [cf. Figs. 3(b) and 3(c)], whose presence poses technical difficulties in evaluating the partition function. In Sec. IV B, we introduce a formal trick by switching on a "magnetic field," such as the term that breaks the rotational symmetry of the problem. The main purpose of this procedure is to isolate the formally diverging contribution of the rotational mode and to restore it afterward in a controlled manner (avoiding the divergences of the partition function). In Secs. IV C and IV D, we finally deal with two different ways to affect the stability of the tilting mode in Fig. 3(c). In Sec. IV C, we do this by imposing a constraint on the unstable mode amplitude and, in Sec. IV D, by implementing an interaction potential at the contact point. These two different procedures lead to identical results in the limit of large forces (homoclinic loop case).

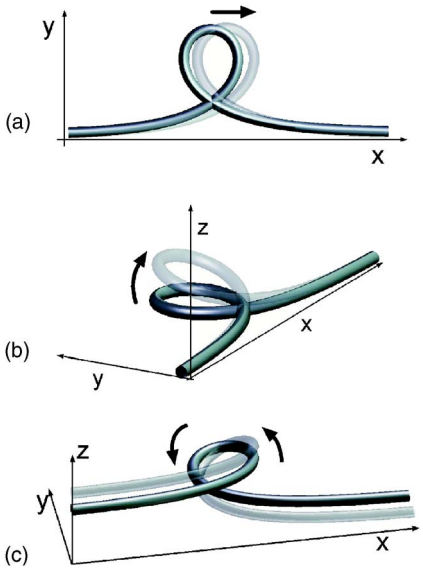


FIG. 3. (Color online) The three discrete eigenmodes in action for $m \approx 1$: (a) The translational mode $\phi_0 = 1/(\sqrt{2}\cosh t)$ [Eq. (31)]. (b) The rotational mode $\vartheta_0 = \sqrt{3/2}\sinh t \cosh^{-2} t$ [Eq. (64)], and (c) the unstable (out of plane tilting) mode $\vartheta_{-1} = \sqrt{3/4}\cosh^{-2} t$ [Eq. (66)].

Despite significant technical subtleties in the calculation, the final results plotted in Fig. 4 and, in particular, the high force limiting case given in Eq. (87), are quite intuitive. They show a renormalization of the effective persistence length in qualitative similarity with the 2D case yet with a different numeric prefactor.

### A. Unstable and rotational zero mode

We first discuss here the relevance of the right parametrization of the unit tangent vector. Beside the fact that our parametrization allows us to deal properly with the measure term, the importance of this choice appears even more evident when considering the 3D loop. Suppose that we study the equilibrium property of DNA pulled by a force in the $z$ direction. The bending energy is

$$E = \int_{-L/2}^{L/2} \left[ \frac{A}{2}(\dot{\phi}^2 \sin^2\theta + \dot{\theta}^2) - F\cos\theta \right] ds, \tag{57}$$

and the saddle point is now $\phi_{\text{loop}} = 0$ and $\theta_{\text{loop}}$ given by Eq. (46) (with $\phi_{\text{loop}}$ replaced by $\theta_{\text{loop}}$). Looking at small variations $\delta\theta$ and $\delta\phi$ around the homoclinic loop solution, we find a *positive definite* second variation of the energy functional,

$$\delta^2 E = \int_{-L/2}^{L/2} \left[ \left( \frac{A}{2}\delta\dot{\theta}^2 + \frac{F}{2}\cos(\theta_{\text{loop}})\delta\theta^2 \right) + A\sin^2(\theta_{\text{loop}})\delta\dot{\phi}^2 \right] ds. \tag{58}$$

This is in striking contradiction to the expected elastic instability of the loop in three dimensions. The reason is that the coordinate system has a singularity at $\theta = 0$, where the $\phi$ angle becomes arbitrary. As explained in Sec. II B, the way to circumvent the problem is to rotate the force direction and to put it along the $x$ axis so that the potential energy part writes now $-F\cos\phi\sin\theta$. In terms of the angles $\phi$ and $\vartheta = \theta - \pi/2$, the energy writes now

$$E[\vartheta, \phi] = \sqrt{AF}\int_{-L/2\lambda}^{L/2\lambda} \left[ \frac{1}{2}(\dot{\phi}^2\cos^2\vartheta + \dot{\vartheta}^2) - \cos\phi\cos\vartheta \right] dt, \tag{59}$$

with the corresponding Euler-Lagrange equations

$$\ddot{\vartheta} = \cos\phi\sin\vartheta - \dot{\phi}^2\cos\vartheta\sin\vartheta,$$

$$\ddot{\phi}\cos^2\vartheta - 2\dot{\phi}\dot{\vartheta}\cos\vartheta\sin\vartheta = \sin\phi\cos\vartheta. \tag{60}$$

We choose in the following the $\vartheta = 0$ solution, i.e., we put the loop into the $x$-$y$ plane. This imposes no restriction because we can always rotate the coordinate system around the $x$ axis to achieve $\vartheta = 0$. In this case, we have $\ddot{\phi} = \sin\phi$, which is the same as Eq. (22), and the saddle point is then given by $\phi_{\text{loop}}(t)$ [cf. Eq. (25)] and $\vartheta_{\text{loop}}(t) = 0$. Then by considering small fluctuations around this saddle point that satisfy Dirichlet boundary, we can again expand Eq. (59) up to second order and obtain

$$\beta E[\delta\vartheta, \phi_{\text{loop}} + \delta\phi] = \beta E_{\text{loop}} + \frac{\beta\sqrt{AF}}{2}\left[ \int_{-L/2\lambda}^{L/2\lambda} \delta\phi(t)\hat{\mathbf{T}}_{\parallel}(t)\delta\phi(t)dt + \int_{-L/2\lambda}^{L/2\lambda} \delta\vartheta(t)\hat{\mathbf{T}}_{\perp}(t)\delta\vartheta(t)dt \right], \tag{61}$$

where the loop energy $E_{\text{loop}}$ and the in-plane fluctuation operator $\hat{\mathbf{T}}_{\parallel}$ are, of course, the same as in the 2D case [cf. Eqs. (27) and (30)], respectively. New, in Eq. (61), is the out-of-plane fluctuation operator $\hat{\mathbf{T}}_{\perp}$ given by

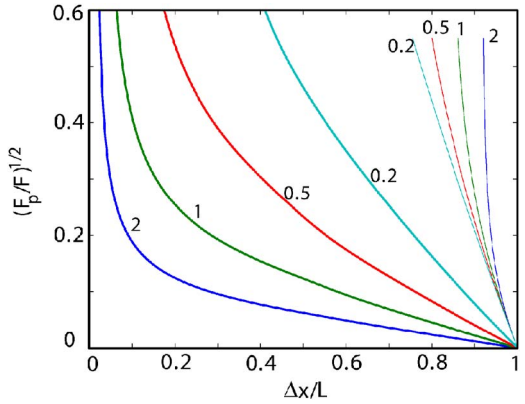


FIG. 4. (Color online) Force-extension curve of a DNA chain under tension with a sliding loop [thick lines, Eq. (81)] and without a loop [thin lines, Eq. (12)] for different ratios $l_p/L$ as denoted by the numbers close to the curves. Specifically, we plot here $(F_p/F)^{1/2}$ with $F_p = k_B T/l_p$ against $\Delta x/L$. In this representation, the curves for loop-free chains collapse in the limit of large forces [cf. Eq. (16)].

$$\hat{\mathbf{T}}_{\perp} = -\frac{\partial^2}{\partial t^2} + 6\,\mathrm{sn}^2\left(\frac{t}{\sqrt{m}}|m\right) - \left(\frac{4+m}{m}\right). \tag{62}$$

Note that with our choice $\vartheta_{\mathrm{loop}}(t)=0$, the measure term does not contribute at this level of the approximation. The main consequence of the quadratic expansion around the saddle-point configuration is that the variables $\vartheta$ and $\phi$ decouple so that the full partition function $Q_{\mathrm{loop}}$ factorizes into the product of the 2D partition function $Q_{2\mathrm{D}}$ [given by Eq. (36)] and the partition function $Q_{\perp}$ accounting for out-of-plane fluctuations

$$Q_{\mathrm{loop}} = Q_{2D} Q_{\perp}. \tag{63}$$

Despite its visual similarity to $\hat{\mathbf{T}}_{\parallel}$ the behavior of the out-of-plane operator $\hat{\mathbf{T}}_{\perp}$ is fundamentally different. The discrete spectrum of $\hat{\mathbf{T}}_{\perp}$ consists of two eigenvalues $\mu_{-1}^{\perp}=-3/m$ and $\mu_0^{\perp}=0$, the first of which is, indeed, negative [42].

The zero eigenvalue mode of $\hat{\mathbf{T}}_{\perp}$ comes from the rotational symmetry around the $x$ axis in a similar manner as the translational invariance of the loop causes a vanishing eigenvalue of $\hat{\mathbf{T}}_{\parallel}$. To compute the contribution of the infinite number of degenerate saddle point related by a rotation around the $x$ axis, we look at infinitesimal rotational transformations of the loop in three dimensions. It is straightforward to show that, up to quadratic order, a rotation of a kink with $\vartheta_{\mathrm{loop}}=0$ around the $x$ axis by a small angle $\varepsilon$ corresponds to the following small changes in $\vartheta_{\mathrm{loop}}$ and $\phi_{\mathrm{loop}}$:

$$\delta\vartheta_{\mathrm{loop}} \approx \varepsilon \sin\phi_{\mathrm{loop}},$$

$$\delta\phi_{\mathrm{loop}} \approx -\frac{1}{2}\varepsilon^2 \sin\phi_{\mathrm{loop}}\cos\phi_{\mathrm{loop}} = O(\varepsilon^2).$$

In the same manner as for the translational zero mode, we first expand $\delta\vartheta(t)$ in a complete set of orthonormal eigenvectors $\vartheta_n(t)$ diagonalizing the operator $\hat{\mathbf{T}}_{\perp}$, i.e., $\delta\vartheta(t)=\Sigma_{n=-1}^{\infty} b_n\vartheta_n(t)$ (the summation starts at $n=-1$ because of the presence of the unstable mode, see below). Next we consider the collective rotation coordinate $0<\varepsilon<2\pi$ as an integration variable in the path integral instead of the normal mode $b_0$ associated to the zero-mode eigenfunction $\vartheta_0(t)$. This change of variable introduces a Jacobian defined by $\partial b_0 = J^{-1}(m)\,\partial\varepsilon$ computed below. We note that in lowest order this rotation leaves $\phi_{\mathrm{loop}}$ unaffected; thus, the same rotation $\delta\vartheta_{\mathrm{loop}}\approx\varepsilon\sin\phi_{\mathrm{loop}}$ can also be generated by the normalized zero-mode eigenfunction

$$\vartheta_0(t) = \left(\int_{-L/2\lambda}^{L/2\lambda} dt\,\sin^2\phi_{\mathrm{loop}}\right)^{-1/2} \sin\phi_{\mathrm{loop}} \tag{64}$$

with $\sin\phi_{\mathrm{loop}}=\mathrm{cn}\left(\frac{t}{\sqrt{m}}\middle|m\right)\mathrm{sn}\left(\frac{t}{\sqrt{m}}\middle|m\right)$. We obviously have $\delta\vartheta_{\mathrm{loop}}\approx\partial b_0\vartheta_0(t)$. By equating the two representations of $\delta\vartheta_{\mathrm{loop}}$, one easily deduces

$$J^{-1}(m) = 2m^{-3/4}\left(\frac{2}{3}\right)^{1/2}[(2-m)E(m)-2(1-m)K(m)]^{1/2}. \tag{65}$$

The expression for $J(m)$ will be necessary for the computation of the out-of-plane determinant later on. In one-dimensional (1D) quantum mechanics, the ground-state wave function has no node, the first excited state wave function has one node, etc. In our case, the wave function $\vartheta_0(t)$ has one node; thus, it cannot be the ground state, and a wave function with no node in the interval considered must exist. It is obviously the eigenfunction of the unstable mode that is given by the (unnormalized) expression

$$\vartheta_{-1}(t) = \mathrm{cn}\left(\frac{t}{\sqrt{m}}|m\right)\mathrm{dn}\left(\frac{t}{\sqrt{m}}|m\right), \tag{66}$$

with the eigenvalue

$$\mu_{-1}^{\perp} = \frac{-3}{m}. \tag{67}$$

This negative eigenvalue makes the 3D loop mechanically unstable. An overview of the three discrete eigenmodes is provided in Fig. 3.

In the following, we will consider several different physical mechanisms to stabilize this mode. In Sec. IV B, we study looped DNA in a strong magnetic field that breaks the rotational invariance and then we enforce the cancellation of the unstable mode either by a geometrical constraint (Sec. IV B) or by an explicit self interaction potential (Sec. IV C).

### B. DNA in a strong magnetic field

A physical situation in which the DNA loop is stabilized is if we switch on a (very strong) magnetic field along the $z$ axis perpendicular to the force direction along the $x$ axis [cf. Fig. 1(d)]. The DNA nucleotides (having $\pi$ electrons) are known to prefer alignment perpendicular to the field, i.e., DNA exhibits a negative diamagnetic anisotropy [29]. The application of a magnetic field $H$ along the z axis drives the DNA molecule into a plane parallel to the $x$-$y$ plane. The total energy of the DNA writes, in this case,

$$E[\vartheta,\phi] = \int_{-L/2}^{L/2}\left[\frac{A}{2}(\dot{\phi}^2\cos^2\vartheta+\dot{\vartheta}^2) - F\cos\phi\cos\vartheta + \frac{\kappa}{2}\sin^2\vartheta\right]ds. \tag{68}$$

The last term gives the coupling between the DNA tangent and the magnetic field $H$, where $\kappa=-\chi_a H^2/h$ characterizes the coupling strength. Here, $\chi_a=\chi_{\parallel}-\chi_{\perp}$ denotes the (experimentally accessible) diamagnetic anisotropy of a single DNA base pair [29], i.e., the difference of the parallel $\chi_{\parallel}$ and perpendicular $\chi_{\perp}$ magnetic susceptibility, respectively. $h=0.34$ nm is the distance between the subsequent DNA base pairs. Note that $\chi_a$ is negative here, i.e., $\kappa>0$ so $\vartheta=0$ is the preferred rod orientation for large $\kappa$.

Expanding $E[\vartheta,\phi]$ up to second order, we obtain the same expression as Eq. (61) except that $\hat{\mathbf{T}}_\perp$ is replaced by a new out-of-plane fluctuation operator $\hat{\mathbf{T}}_\perp^\kappa$

$$\hat{\mathbf{T}}_\perp^\kappa = \left[ -\frac{\partial^2}{\partial t^2} + 6\,\mathrm{sn}^2\left(\frac{t}{\sqrt{m}}|m\right) - \left(\frac{4+m}{m}\right) + \frac{\kappa}{F}\right]. \quad (69)$$

The spectrum of Eq. (69) is given by shifting the spectrum of $\hat{\mathbf{T}}_\perp$ by the constant $\kappa/F$, leading to the eigenvalues $\mu_s^\kappa = \mu_s^\perp + \kappa/F$. The rotational mode is immediately destroyed for any nonzero coupling constant $\kappa > 0$. More importantly, the previously unstable mode $\vartheta_{-1}$ now becomes stable provided that $\kappa/F > 3$, i.e., for $\kappa > \kappa_{\mathrm{crit}} = 3F$. As the partition function factorizes into the product of the 2D partition function and an out-of-plane contribution, we only need to compute the determinant associated with the fluctuation operator (69), which is given in Eq. (B12), for the case $L/2\lambda \gg 1$. From this, we obtain

$$Q_\perp^\kappa = \sqrt{\frac{\beta\sqrt{AF}c(c+2)(c+1)}{\pi(c-2)(c-1)}}e^{-c(L/2\lambda)} \quad (70)$$

with $c = \sqrt{1+\kappa/F}$. The free energy $\beta G = -\ln(Q_{2D}Q_\perp)$ with $Q_{2D}$ given by Eq. (49) has the following form:

$$\beta G = -\beta FL + 8\beta\sqrt{FA} + \frac{\left(1+\sqrt{1+\frac{\kappa}{F}}\right)L\sqrt{F/A}}{2} - \ln\left(\sqrt{\frac{2c(c+2)(c+1)}{(c-2)(c-1)}}\frac{LA^{1/4}}{\pi^{3/2}\beta^{3/2}}F^{5/4}\right). \quad (71)$$

Differentiating this expression with respect to $F$ leads to the force-extension relation for all forces $F < \kappa/3$. Since this turns out to be a lengthy expression, we give, here, only the result for the limiting case $\kappa \gg F$ (and, as assumed above, $L/2\lambda \gg 1$)

$$\frac{\langle \Delta x\rangle}{L} = 1 - \frac{1}{4\beta}\sqrt{\frac{1}{A\kappa}} - \frac{1}{\beta\sqrt{AF}}\left[\frac{1}{4} + 4\frac{l_P}{L} - \frac{1}{8}\left(\frac{F}{\kappa}\right)^{3/2} + O\left(\frac{F}{\kappa}\right)^{5/2}\right] + O\left(\frac{1}{\beta FL}\right). \quad (72)$$

This expression is similar to the 2D case [Eq. (52)], which is related to the fact that we assume a strong cost for out-of-plane fluctuations by setting $\kappa \gg F$. The major contribution from the out-of-plane fluctuations is the second term on the right-hand side of Eq. (72) that describes an effective $F$-independent shortening of the contour length. The next-order $\kappa$-dependent correction is already by a factor $F/\kappa$ smaller and, therefore, negligible.

Finally, could we experimentally observe the force extension curve derived above? Unfortunately, the coupling parameter $\kappa$ turns out to be too small for reasonable magnetic fields [44] to be of physical relevance in practice, i.e., $\kappa \ll 3F$. Nevertheless, the formal diamagnetic term $\kappa \sin^2\vartheta$ introduced in Eq. (68) is conceptually useful to understand the (otherwise unstable) behavior of the DNA loop in three dimensions. It also turns out to be technically convenient to use an infinitesimally small "diamagnetic term" in order to break (and restore in a controlled fashion) the rotational symmetry. This procedure allows the computation of the 3D determinant and cancels the formally diverging contribution of the rotational zero mode (cf. Appendix A).

### C. Force-extension with a geometrical constraint

In this section, we compute the partition function of looped DNA by forcing the mean tangent of the loop to stay in a plane, which is the simplest stabilizing procedure. This geometrical constraint corresponds to applying forces at the two-chain termini that maintain them in-plane. The constraint is implemented by the introduction of a $\delta$ Dirac distribution in the partition function; thus, the out-of-plane partition function in the presence of a external magnetic field becomes

$$Q_\perp^\kappa = \int \delta\left(\frac{\lambda}{L}\int_{-L/2\lambda}^{L/2\lambda}\delta\vartheta dt\right)e^{-(\beta\sqrt{AF}/2)\int_{-L/2\lambda}^{L/2\lambda}\delta\vartheta\hat{\mathbf{T}}_\perp^\kappa\delta\vartheta dt}\mathcal{D}[\delta\vartheta]. \quad (73)$$

The formal presence of the external magnetic field is necessary because the rotational mode $\vartheta_0$ corresponds to a zero eigenvalue and causes a divergence of the partition function $Q_\perp^{\kappa=0}$. The problem results from the fact that a rotation of the kink around the $x$ axis costs no energy, and consequently, the entropic contribution of this state space direction seems to diverge (within the Gaussian approximation implied by the saddle-point approximation used here). To circumvent this problem, we employ the following trick. Instead of $\hat{\mathbf{T}}_\perp$ we use $\hat{\mathbf{T}}_\perp^\kappa$ from Eq. (69) and after performing all other calculations we let $\kappa \to 0$ (note that $\hat{\mathbf{T}}_\perp^\kappa|_{\kappa=0} \equiv \hat{\mathbf{T}}_\perp$). Physically, this procedure corresponds to infinitesimally breaking the rotational symmetry (around the force direction) and restoring it afterward in a controlled manner in the limit $\kappa \to 0$.

Physically, it is clear that the main contribution of the mean value of the tilting angle defined by

$$\langle \delta\vartheta\rangle = \frac{\lambda}{L}\int_{-L/2\lambda}^{L/2\lambda}\delta\vartheta dt \quad (74)$$

comes from the unstable mode that induces the large out-of-plane deviation. The contribution from the rest of the eigenmodes is small and stable, so that the eigenmode expansion $\langle\delta\vartheta\rangle = \Sigma_{n=-1}^{\infty} b_n\langle\vartheta_n\rangle$ can be approximated by

$$\langle\delta\vartheta\rangle \approx b_{-1}\langle\vartheta_{-1}\rangle = b_{-1}\sqrt{\frac{3}{2}}\frac{m^{1/4}}{K(m)[(1+m)E(m)-(1-m)K(m)]^{1/2}}. \quad (75)$$

In this way, we approximate the constraint in Eq. (73) by a constraint that fixes the mean out-of-plane deviation induced by the unstable mode alone to zero. It means that we relax a bit the constraint in Eq. (73) by allowing the other modes to induce nonzero mean value of the tilting angle. This contribution, however, will be small and limited by the positive spring constants of the stable out of plane modes.

Using Eq. (75), it is straightforward to rewrite Eq. (73) as follows:

$$Q_{\perp}^{\kappa} = i2\sqrt{|\mu_{-1}|}\sqrt{\frac{\beta\sqrt{AF}}{2\pi}} \times\left(\frac{1}{\langle\vartheta_{-1}\rangle}\int_{-\infty}^{\infty} e^{-(\beta\sqrt{AF}/2)\mu_{-1}b_{-1}^2}\delta(b_{-1})db_{-1}\right) \times\sqrt{\frac{\beta\sqrt{AF}}{2\pi D_{\perp}^{\kappa}\left(-\frac{L}{2\lambda},\frac{L}{2\lambda}\right)}}, \tag{76}$$

where—with $\kappa$ being small—the determinant is now imaginary. Note that by removing the unstable mode from the determinant we have taken into account that the Gaussian integral of the unstable mode is given by

$$\int_{-\infty}^{\infty} e^{-\mu_{-1}x^2/2}\frac{dx}{\sqrt{2\pi}} \equiv \frac{i}{2\sqrt{|\mu_{-1}|}}$$

and not by $i/\sqrt{|\mu_{-1}|}$ as a naive analytical continuation would suggest (see, for instance, [23] Chap. 17, or [45]). Expression (76) shows that one cannot simply remove the unstable mode from the determinant, but one has to replace it carefully by introducing a correct constraint expression in the partition function. For instance, canceling simply the unstable mode would introduce nonphysical divergences in the limit of very small forces.

We are only interested here in the limit of zero magnetic field. In order to restore the rotational invariance, we have to deal with the rotational zero mode by dividing out the would-be-zero mode $\mu_0(\kappa)$ and replacing it by the real physical space it populates. Therefore we have to compute the $\kappa$-independent partition function $Q_{\perp}$ defined by

$$Q_{\perp} = \lim_{\kappa\to 0}\sqrt{2\pi\mu_0(\kappa)\beta\sqrt{AF}}J^{-1}(m)Q_{\perp}^{\kappa}, \tag{77}$$

where we have replaced the integration on the normal mode $b_0$ by the collective coordinate $\varepsilon$ whose integration domain is finite and equal to $2\pi$. The Jacobian is given by Eq. (65) and $\mu_0(\kappa)=\kappa/F$.

The out-of-plane determinant can be deduced from the Gelfand-Yaglom method, which specifies that the determinant can be obtained from the solution of the following generalized second-order Lamé equation:

$$\left(\hat{\mathbf{T}}_{\perp} + \frac{\kappa}{F}\right)y(t) = 0. \tag{78}$$

The determinant is then given by the relation $D_{\perp}^{\kappa}(-L/2\lambda, L/2\lambda)=y(L/2\lambda)$, valid when the conditions $y(-L/2\lambda)=0$ and $\dot{y}(-L/2\lambda)=1$ are satisfied [42]. A detailed determination of the solution of Eq. (78) is provided in Appendix A. In the small $\kappa$ limit the out-of-plane determinant admits the following expansion [cf. Eq. (A36)]:

$$D_{\perp}^{\kappa}\left(-\frac{L}{2\lambda},\frac{L}{2\lambda}\right) = -\frac{\kappa}{F}\frac{2}{3\sqrt{m}(1-m)} \times[(2-m)E(m)-2(1-m)K(m)], \tag{79}$$

which is formally negative because of the presence of the unstable mode. Combining the different contributions in Eq. (77), we arrive at the following expression for the out-of-plane partition function:

$$Q_{\perp} = \frac{2\sqrt{2}}{\sqrt{\pi}}\left(\frac{l_p}{L}\right)^{3/2}K(m)^{5/2}(1-m)^{1/2} \times\left(\frac{(1+m)E(m)-(1-m)K(m)}{m}\right)^{1/2}. \tag{80}$$

The complete semiclassical partition function of the looped DNA in three dimensions is then given by $Q_{\text{loop}}=Q_{2D}Q_{\perp}$ with $Q_{2D}$ given by Eq. (36).

The mean end-to-end distance has now four contributions

$$\langle\Delta x\rangle = \langle\Delta_{\text{E}}x\rangle + \langle\Delta_{\parallel}x\rangle + \langle\Delta_{\text{err}}x\rangle + \langle\Delta_{\perp}x\rangle, \tag{81}$$

where the first three expressions are given by Eqs. (38)–(40) and the out-of-plane contribution obeys

$$\langle\Delta_{\perp}x\rangle = \frac{L^2}{16l_p m K^2(m)E(m)}\left(\frac{5(1+m)E^2(m)-2(6-3m-m^2)K(m)E(m)+(7-12m+5m^2)K^2}{(1+m)E(m)-(1-m)K(m)}\right). \tag{82}$$

With the complete analytical expression at hand, it is straightforward to compute force-extension curves (some examples for different ratios $L/l_p$ can be found in Fig. 4). The curves show clearly different scaling behavior for low and strong forces. In the small $m$ limit, $(L/\lambda \ll 1)$—corresponding to the case $L<l_p$—Eq. (82) has the following expansion:

$$\langle\Delta_{\perp}x\rangle \approx \frac{L^2}{16\pi^2 l_p}[1+O(m)], \tag{83}$$

which has the same scaling as the in-plane fluctuation contribution Eq. (43).

In the limit $L/\lambda\to\infty$ or $m\to 1$, the out-of-plane partition function [Eq. (80)] takes the following form:

$$Q_{\perp} \approx \frac{8\sqrt{2}}{\sqrt{\pi}}(\beta\sqrt{F})^{5/4}l_p^{1/4}e^{-L/2\sqrt{F/A}}, \tag{84}$$

which leads to the force-extension curve

$$\langle \Delta_\perp x \rangle \approx -\frac{L}{4}\sqrt{\frac{k_B T}{F l_P}} + \frac{5k_B T}{4F}. \tag{85}$$

When adding this result to the contributions stemming from the 2D computation, we finally obtain

$$\langle \Delta x \rangle = L - \frac{1}{2}\sqrt{\frac{k_B T}{F l_P}}L - 4\sqrt{\frac{k_B T l_P}{F}} + \frac{9k_B T}{4F}, \tag{86}$$

which can also be written as

$$\frac{\langle \Delta x \rangle}{L} = 1 - \frac{1}{2}\left(1 + 8\frac{l_P}{L}\right)\frac{1}{\beta\sqrt{AF}} + \frac{9}{4\beta F L}. \tag{87}$$

in order to facilitate the comparison with Eq. (52) of the 2D case.

In Sec. IV D, we compute the force-extension curve in the strong force regime with a loop stabilized by a self-attractive potential. This computation allows us to check, explicitly, that the force-extension relation is fairly independent of the details of the stabilizing procedure and a much more physical loop-stabilization leads again to Eq. (86).

### D. DNA Self-attraction and the homoclinic loop

Now we treat an experimentally relevant case in which a loop is stabilized in three dimensions: self-attracting DNA. DNA is known to effectively attract itself in many solvents despite its strong negative bare charge. Typical situations inducing DNA self-attraction are poor solvents (such as alcohol), small neutral polymers (such as PEG), the presence of multivalent counterions (such as CoHex and Spermidine), or small cationic proteins acting as linkers between two DNA surfaces. Indeed, it was a single-molecule stretching experiment on DNA condensed with multivalent counterions [14] that made us think about the force response of loops. Another important situation of effective DNA self-attraction is given when sliding protein linkers like condensin stabilize loops via topological catenation with DNA [46].

How should we deal with the DNA self-interaction? A formal treatment that first comes to mind is to introduce a potential $V(\|\underline{x}(s_1)-\underline{x}(s_2)\|)$ acting between any pair of points $s_1$ and $s_2$ on the DNA molecule and to write the total interaction energy in form of a double integral (over $s_1$ and $s_2$) as an additional term in our Hamiltonian. The problem is, however, that we describe the DNA conformation here by the two spherical angles ($\vartheta$ and $\phi$) of its *tangent* vector, whereas the self-interaction acts in *real space* ("integrated tangent space"). This makes such a Hamiltonian virtually intractable, and hence, we need a reasonable simplification of the DNA self-attraction.

To this end, we make two simplifying assumptions: (i) There is only *a single discrete* DNA self-contact point, given by the crossing point of the homoclinic loop solution, and (ii) the interaction potential $V(\|\underline{x}(s_1)-\underline{x}(s_2)\|)$ is *short ranged* enough so that the interaction energy at the crossing becomes independent of the crossing angle, i.e., other parts of the DNA (apart from the crossing point) do not interact with each other.

These fairly reasonable assumptions imply that the loop ground-state solution will not be significantly modified by the self-attraction, and only the fluctuations around it will be affected. This means that we can write the (linearized) loop energy around the solution $\vartheta=0, \phi=\phi_{\text{loop}}$ in a way similar to in Sec. IV C, namely,

$$E[\delta\vartheta, \phi_{\text{loop}} + \delta\phi] = E_{\text{loop}} + \frac{\sqrt{AF}}{2}\int_{-L/2\lambda}^{L/2\lambda} \delta\phi \hat{\mathbf{T}}_\parallel \delta\phi dt + \frac{\sqrt{AF}}{2}\int_{-L/2\lambda}^{L/2\lambda} \delta\vartheta \hat{\mathbf{T}}_\perp^\kappa \delta\vartheta dt + V[D_c(\delta\vartheta)]. \tag{88}$$

The last term $V(D_c)$ that we introduced here, in accordance with above-stated assumptions, represents the interaction potential of two overcrossing parts of DNA that have a closest distance $D_c$. To keep the problem tractable, we approximate the distance $D_c$ by the *perpendicular distance* of the two crossing DNA parts at the *equilibrium (mean) crossing point* $t_c$ of the homoclinic loop

$$D_c(\delta\vartheta) \approx \lambda\int_{-t_c}^{t_c} \sin\delta\vartheta(t)dt \approx \lambda\int_{-t_c}^{t_c}\delta\vartheta(t)dt. \tag{89}$$

The crossing point $t_c$ will be given by the (in-plane) projected self-crossing of the loop. This implies the condition that the integral (over the interval $[-t_c, t_c]$) of the out of plane component of the loop tangent vanishes, i.e., $\int_{-t_c}^{t_c}\cos\phi_{\text{loop}}(t)dt=0$, which leads to the following implicit equation for $t_c$:

$$t_c = \sqrt{m}\frac{E(t_c/\sqrt{m}|m)}{1-m}. \tag{90}$$

Before we compute further, it is interesting to have a short look at $D_c$ from Eq. (89). Because $D_c$ depends only on the out-of-plane perturbations, $\delta\vartheta$, the in-plane ($\delta\phi$) problem stays unaffected. Note further that the out-of-plane rotational mode $\vartheta_0$ (the generator of an infinitesimal rotation) leaves the distance $D_c$ unaffected: formally, because $\vartheta_0(t)$ is an odd function and, physically, because rotations leave distances fixed.

Now the partition function resulting from Eq. (88) for any given $V$ can be written as follows:

$$Q^V = Q_{2D}Q_\perp^V. \tag{91}$$

Only the out-of-plane partition function $Q_\perp^V$ is modified by the presence of the contact potential and is given by

$$Q_\perp^V = \int_{-\infty}^{\infty} e^{-\beta V(2t_c\lambda\vartheta_c)}Q_\perp(\vartheta_c)d\vartheta_c, \tag{92}$$

where we introduce the dimensionless angular variable $\vartheta_c = D_c/2t_c\lambda$ that visually corresponds to a "opening angle" of the loop. The expression $Q_\perp(\vartheta_c)$ denotes the constrained partition function

$$Q_\perp(\vartheta_c) = \int \delta\left(\vartheta_c - \frac{1}{2t_c}\int_{-t_c}^{t_c}\delta\vartheta dt\right) \times e^{-(\beta\sqrt{AF}/2)\int_{-L/2\lambda}^{L/2\lambda}\delta\vartheta\hat{\mathbf{T}}^\kappa{}_\perp\delta\vartheta dt}\mathcal{D}[\delta\vartheta]. \tag{93}$$

To compute this path integral, we replace the $\delta$ function by its Fourier representation

$$\delta\left(\vartheta_c - \frac{1}{2t_c}\int_{-t_c}^{t_c}\delta\vartheta dt\right) = \frac{1}{2\pi}\int_{-\infty}^{\infty} e^{ip(\vartheta_c-(1/2t_c)\int_{-t_c}^{t_c}\delta\vartheta dt)}dp. \tag{94}$$

The integral in the exponent is more elegantly written as a scalar product of $\delta\vartheta$ with a "boxcar" function $\Pi(t)=H(t+t_c)-H(t-t_c)$ with $[H(x)=1$ for $x>0$, $H(x)=1/2$ for $x=0$ and $H(x)=0$ otherwise],

$$\int_{-t_c}^{t_c}\delta\vartheta dt = \int_{-L/2\lambda}^{L/2\lambda}\Pi(t)\delta\vartheta(t)dt = \langle\Pi|\delta\vartheta\rangle, \tag{95}$$

where we introduced the scalar product $\langle f|g\rangle = \int_{-L/2\lambda}^{L/2\lambda} f(t)g(t)dt$. In this notation and by virtue of Eqs. (94) and (95), the partition function $Q_\perp(\vartheta_c)$ [Eq. (93)] can be recast in a more transparent form,

$$Q_\perp(\vartheta_c) = \frac{1}{2\pi}\int_{-\infty}^{\infty} e^{ip\vartheta_c} \times \int e^{-(\beta\sqrt{AF}/2)\langle\delta\vartheta|\hat{\mathbf{T}}_\perp|\delta\vartheta\rangle - i(p/2t_c)\langle\Pi|\delta\vartheta\rangle}\mathcal{D}[\delta\vartheta]dp. \tag{96}$$

We have now to compute the following path integral:

$$\hat{Q}_\perp^\kappa(p) = \int e^{-(\beta\sqrt{AF}/2)\langle\delta\vartheta|\hat{\mathbf{T}}_\perp^\kappa|\delta\vartheta\rangle - i(p/2t_c)\langle\Pi|\delta\vartheta\rangle}\mathcal{D}[\delta\vartheta]. \tag{97}$$

This path integral can be rewritten as a Gaussian path integral in the presence of an external source $j(p,t)=ip\Pi(t)$ coupled linearly to the fluctuating field $\delta\vartheta$. We refer to Appendix B for the computation of this kind of path integral. The important point is that it can be written in the form [see Eq. (B8)]

$$\hat{Q}_\perp^\kappa(p) = \sqrt{\frac{\beta\sqrt{AF}}{2\pi D_\perp^\kappa\left(-\frac{L}{2\lambda},\frac{L}{2\lambda}\right)}}e^{-\beta E[j]}, \tag{98}$$

where the determinant $D_\perp^\kappa\left(-\frac{L}{2\lambda},\frac{L}{2\lambda}\right)$ is independent of the source term. The energy term $E[j]$ is given by Eq. (B19) (with the action $S$ replaced by energy $E$).

Along similar lines as in Eq. (77), we go to the limit $\kappa\to 0$

$$\hat{Q}_\perp(p) \underset{\kappa\to 0}{=} \sqrt{2\pi\mu_0(\kappa)\beta\sqrt{AF}}J^{-1}(m)\hat{Q}_\perp^\kappa(p), \tag{99}$$

where the Jacobian is given by expression (65).

It is a very difficult task to calculate Eq. (98) for the case of a finite chain length, so that we restrict ourself to the limit of very long chains. In this case, the determinant is given by Eq. (B12) and the functional $E[j]$ by Eq. (B20) which is

$$\beta E[j] = -\frac{3}{32}\frac{(3t_c^2-10)}{\beta t_c\sqrt{AF}}p^2. \tag{100}$$

The implicit condition on $t_c$ [Eq. (90)] becomes in this limiting case

$$t_c = 2\tanh t_c, \tag{101}$$

which has $t_c\approx 1.915$ as the numeric solution. This corresponds to the actual loop circumference of $2\times 1.915\lambda$. The Jacobian equation (65) in this limiting case obeys $J^{-1}(m=1)=2\sqrt{2/3}$. Using the fact that the zero eigenvalue can be written as $\mu_0(\kappa)=\frac{\kappa}{F}$, we can compute the partition function (99) in the infinite long molecule limit for $\kappa\to 0$,

$$\hat{Q}_\perp(p) = i8\left(\frac{l_P}{\lambda}\right)e^{-(L/2\lambda)}e^{(3\lambda/32l_Pt_c)(3t_c^2-10)p^2}. \tag{102}$$

Note that, because of the unstable mode, $\hat{Q}_\perp$ is imaginary. Transforming back into real space yields

$$Q_\perp(\vartheta_c) = \frac{1}{2\pi}\int_{-\infty}^{\infty} e^{ip\vartheta_c}\hat{Q}_\perp(p)dp = 8\sqrt{\frac{\Gamma}{\pi}}\left(\frac{l_P}{\lambda}\right)^{3/2}e^{-(L/2\lambda)}\exp\left[4t_c^2\Gamma\frac{l_P}{\lambda}(\vartheta_c)^2\right], \tag{103}$$

where we introduced the scale-independent (negative) elasticity constant for the out-of-plane tilting

$$\Gamma = \frac{2}{3t_c(3t_c^2-10)}. \tag{104}$$

The result in Eq. (103) indicates that the larger the perpendicular distance $D_c$ (and equivalently the angle $\vartheta_c=D_c/2t_c\lambda$), the larger the partition function. This is intuitively clear as the system without the constraint, "$D_c$=const." is intrinsically unstable tending to increase the distance $D_c$.

Using Eq. (92), we can deduce for any given potential $V(z)$ the out-of-plane partition function

$$Q_\perp^V = \frac{8}{\lambda}\sqrt{\frac{\Gamma}{\pi}}\left(\frac{l_P}{\lambda}\right)^{3/2}e^{-(L/2\lambda)}\int_{-\infty}^{\infty} e^{\Gamma(l_P/\lambda)(z/\lambda)^2-\beta V(z)}dz. \tag{105}$$

We can now deduce the full partition function $Q^V$ by combining Eqs. (49), (91), and (105)

$$Q^V = \frac{32\sqrt{\Gamma}Ll_P^{5/2}}{\pi^{3/2}\lambda^{5/2}}e^{\beta FL-8(l_P/\lambda)-(L/\lambda)}\int_{-\infty}^{\infty} e^{\Gamma(l_P/\lambda)(z/\lambda)^2-\beta V(z)}dz. \tag{106}$$

This expression has to be taken seriously only for sufficiently fast-growing interaction potentials $V(z)$ for which the integral above stays finite. Otherwise, the system is metastable and the integral diverges. But even in the case when the bound state, say $z=z_0$, is just a local metastable state the integral above $Q^V$ still makes some sense if the $V(z)$ is very deep. In this case, the system can be considered as being in quasi equilibrium (on some experimentally relevant time

scale). If, for instance, we approximate $V(z)$ locally by a quadratic potential $V(z)=\frac{1}{2}K(z-z_0)^2$, we obtain

$$Q^V = \frac{32\sqrt{2\Gamma}Ll_P^{5/2}}{\pi\lambda^3\sqrt{\beta\lambda^3K-2\Gamma l_P}}e^{[\Gamma\beta Kl_P/(\lambda^3\beta K-2\Gamma l_P)]z_0^2}e^{\beta FL-8(l_P/\lambda)-(L/\lambda)}$$
$$\approx \frac{32\sqrt{2\Gamma}Ll_P^{5/2}}{\pi\lambda^{9/2}\sqrt{\beta K}}e^{(\Gamma l_P/\lambda^3)z_0^2}e^{\beta FL-8(l_P/\lambda)-(L/\lambda)}. \quad (107)$$

The last expression is valid in the limit of strong localization, $K\lambda^2 \gg \sqrt{AF}$, i.e., $K \gg F^{3/2}A^{-1/2}$. For piconewton forces and DNA stiffness $A=50k_BTnm$, this corresponds to $K \gg 0.1$ pN/nm, a condition easily satisfied even by a strongly screened electrostatic interaction, i.e., a multivalent counterion mediated cross-link.

Let us finally write the force-extension relation resulting from the general expression Eq. (106). We express the free energy $G^V=-\beta^{-1}\ln Q^V$ in terms of $F$ and $A$ (instead of $\lambda=\sqrt{A/F}$),

$$\beta G^V = -\beta FL + (L+8l_P)\sqrt{\frac{F}{A}} - \ln\left(\frac{1}{L}\int_{-\infty}^{\infty} e^{\beta\Gamma A^{-1/2}F^{3/2}z^2-\beta V(z)}dz\right) - \ln\left(\frac{32\sqrt{\Gamma}L^2\beta^{5/2}A^{1/4}F^{9/4}}{\pi^{3/2}}\right). \quad (108)$$

This leads to the force extension relation

$$\frac{\langle\Delta x\rangle}{L} = 1-\frac{1}{2}\left(1+8\frac{l_P}{L}\right)\frac{1}{\beta\sqrt{AF}}+\frac{9}{4\beta FL} + \frac{3\Gamma}{2}\frac{1}{L\lambda}\frac{\int_{-\infty}^{\infty} z^2 e^{\beta\Gamma A^{-1/2}F^{3/2}z^2-\beta V(z)}dz}{\int_{-\infty}^{\infty} e^{\beta\Gamma A^{-1/2}F^{3/2}z^2-\beta V(z)}dz}. \quad (109)$$

The last term $\sim\langle D_c^2\rangle/(L\lambda)$ is negligibly small because $\langle D_c^2\rangle$ scales typically as the squared polymer cross section (for a short-ranged surface-contact interaction). In the most extreme case, the contact distance $D_c$ could become comparable to $\lambda$ (the loop head size), i.e., $\langle D_c^2\rangle \lesssim \lambda^2$, but the latter is still much smaller than $L\lambda$. That means that (for reasonable parameters of $F$ and $L$) the force extension relation of a DNA loop with attractive contact interaction will essentially be independent of the concrete realization of the self-interaction potential $V(x)$ and we recover the result of Eq. (86). The last term $O[(\beta FL)^{-1}]$ is always negligible for large forces, and therefore, the average extension is to a good approximation given by the first two terms of Eq. (109),

$$\frac{\langle\Delta x\rangle}{L} \approx 1-\frac{1}{2}\left(1+8\frac{l_P}{L}\right)\frac{1}{\beta\sqrt{AF}}. \quad (110)$$

The second term is the usual "straight WLC" fluctuation contribution in three dimensions [Eq. (16)]; the last term is the force extension signature of the DNA loop [cf. also Eq. (52)].

## V. APPLICATIONS

### A. Single loop

The computations performed in Sec. IV show that the force-extension relation of looped DNA is fairly independent of many details, such as how the loop is stabilized in three dimensions. Furthermore, the shape fluctuations and the loop itself contribute additively to the reduction of the end-to-end distance $\langle\Delta x\rangle$ [cf. Eq. (110)], whereas coupling terms are on the order $(\beta FL)^{-1}$ and, therefore, negligible in the experimentally relevant regime of large forces. Since both relevant contributions in Eq. (110) have a $F^{-1/2}$ scaling looped DNA features the same functional form as the usual WLC expression [Eq. (16)] but with an *apparent* persistence length

$$l_P^{\text{app}} = \frac{l_P}{\left(1+8\frac{l_P}{L}\right)^2} \quad (111)$$

that is Eq. (1) of the Introduction. One has thus to be cautious when one infers the stiffness of a looped chain from a stretching experiment: If the chain is not *much* longer than its persistence length, then the chain appears to be softer than it really is. For example, for $L/l_P=10$, one finds $l_P^{\text{app}} \approx 0.31l_P$ and, for $L/l_P=50$, there is still a remarkable effect, namely, $l_P^{\text{app}} \approx 0.74l_P$.

DNA with a sliding loop can be considered as a paradigmatic example for fluctuations around a nontrivial ground state that renders analytical calculation possible. But do sliding loops remain just an academic toy model or are there any experimental systems that feature DNA with sliding loops? Recent experiments suggest that condensin, a protein that is involved in DNA compaction during mitosis, might induce sliding loops on DNA [47]. In fact, a ring made from two condensin units might act as a loop fastener [46] that stabilizes a loop on DNA. Strick *et al.* [47] have studied DNA under tension in the presence of condensin. These experiments show that DNA compactifies dramatically on addition of condensin in the presence of adenosine triphosphate (ATP). The experiments indicate that many condensins act collectively (e.g., it turned out to be not possible to study single compaction events by simply going to low condensin concentrations). Only in the presence of competitor DNA, single compaction steps on the DNA chain under tension could be resolved. The typical size of a compaction step for the DNA chain under a tension of $F=0.4$ pN was $\sim$85 nm. Our theoretical prediction is that the formation of a loop under that force leads to a reduction of 90 nm [cf. the third term on the right-hand side of Eq. (110)]. Also, rupture events under a much higher force of 10 pN were studied and a pronounced peak $\sim$30 nm length release has been found; our theory predicts a loop size of 18 nm under that tension. Our comparison to the experiments does not allow a definite conclusion, but the numbers indicate the picture of a sliding loop to be compatible with the experimental findings on DNA-condensin complexation.

### B. Protein-induced kink

As pointed out in Ref. [25] one can use the insight gained in the homoclinic loop calculation to derive the elastic response of a number of other experimentally relevant situations. Consider, for instance, a DNA chain under tension that features a kink with a fixed deflection angle $\alpha$ as it might be induced by a bound protein. The ground-state configuration is then given by symmetrically cutting out a piece of the homoclinic shape in the center and gluing together of the two resulting pieces. Another related example is the pulling of a chain via an AFM tip from a surface to which it is adsorbed. In this case again, the resulting shape of the chain can be constructed from pieces of the homoclinic configuration [25]. In both cases, the mapping of the deflected DNA (and its elastic response) onto a part of a loop is possible because of the negligible contribution of the zero mode to the force extension relation (as the computations above show in the limit of large forces).

Also in these cases, we expect that a decomposition into elastic and entropic contributions, similarly to Eq. (110), holds. Under this assumption, it is then straightforward to calculate the force-extension response of DNA with a localized deflection as

$$\frac{\langle \Delta x \rangle}{L} \approx 1 - \frac{1}{2}\left(1 + C(\alpha)\frac{l_P}{L}\right)\frac{1}{\beta\sqrt{AF}}, \tag{112}$$

where $C(\alpha)$ is a geometric coefficient that depends on the deflection angle $\alpha$

$$C(\alpha) = 8\left[1 - \cos\left(\frac{\alpha}{4}\right)\right] \tag{113}$$

As for the loop case, we can interpret Eq. (112) in terms of a reduced apparent persistence length

$$l_P^{\mathrm{app}}(\alpha) = \frac{l_P}{\left[1 + C(\alpha)\frac{l_P}{L}\right]^2}. \tag{114}$$

A trivial case is $\alpha=0$ that corresponds to unkinked DNA, where $l_P^{\mathrm{app}}=l_P$. Another special case is $\alpha=2\pi$ corresponding to a full revolution deflection (i.e., a loop). Then, $C(\alpha)=8$ and Eq. (114) becomes, indeed, Eq. (111). For the case of AFM stretching, one obtains a similar geometric term (cf. Ref. [25]).

An important application of Eq. (114) is the possibility to determine the deflection angle generated by a DNA-bound protein from single-molecule stretching experiments [25]. An example for such a protein is the GalR complex, where the opening angle is not known. However, there are some indications for the "antiparallel" configuration (i.e., $\alpha \approx \pi$ [26,48]). With Eqs. (112) and (114) at hand, one can predict the loss of length due to the binding of a GalR complex with the conjectured angle $\alpha=\pi$. For the force $F=0.88$ pN applied in the experiment [26] with a fixed loop of size 38 nm, Eqs. (112) and (114) predict a loss of length of 56 nm (with the DNA hidden inside the fixed loop included). This corresponds to the experimental value 55 nm±5 nm [26]. Thus, these findings strongly support the antiparallel loop model.

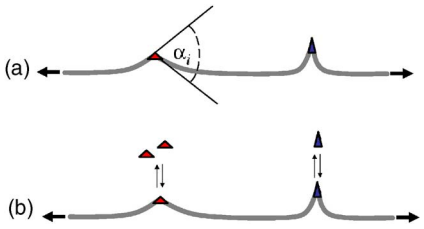


FIG. 5. (Color online) Stretching DNA with kink-generating proteins. The time scales for the free exchange of the proteins with the solution are (a) much longer or (b) much shorter than the experimental time scale. For large forces (a) exibits a large renormalization of $l_P$ [cf. Eq. (115)], whereas in (b), there is asymptotically no renormalisation [Eqs. (116) and (117)].

### C. Many loops or kinks

Up to know we considered the elastic response of single loops and kinks. In this section, we generalize to the case when many loops or kinks are bound to a single DNA chain under tension. Let us first consider the case of a fixed number of loops and/or kinks. Denote by $N_i$ the number of proteins of species $i$ bound to the DNA chain, each inducing a deflection angle $\alpha_i$ with a resulting line density $\rho_i=N_i/L$; this includes again the special case of a loop where $\alpha=2\pi$. We restrain ourselves to the case where the mean distance between kinks and loops along the DNA chain is much larger than their typical size, i.e., where $\lambda\rho \ll 1$ with $\rho=\Sigma_i\rho_i$, denoting the overall line density of bound proteins. In many cases, one can then assume that the contribution of each bound protein to the reduction of the end-to-end distance is independent of the presence of the other proteins. Generalizing Eqs. (112) and (114) to this situation, we obtain

$$l_P^{\mathrm{app}} = \frac{l_P}{\left[1 + l_P\sum_i C(\alpha_i)\rho_i\right]^2}. \tag{115}$$

Equation (115) shows, not unexpectedly, that an increase of the loop and/or kink density manifests itself in a decrease of $l_P^{\mathrm{app}}$. This equation is asymptotically valid for any number of loops and kinks provided that the stretching force is large enough to meet the dilute "gas of defects" approximation, i.e., for $\lambda\rho=\rho\sqrt{A/F} \ll 1$. In the dense regime (weak forces), the defects start to interact and Eq. (115) does not hold anymore. This regime is beyond the scope of the present work.

We note that a previous numerical study [22] of a discretised version of the WLC with local kinks presented numerical results of force-extension relation for DNA with equally spaced $\alpha=90°$ kinks (cf. Fig. 5 in [22]). These curves showed a shift in the force-extension curve that can indeed be described by change of the apparent persistence length given by Eq. (115). We predict $l_P^{\mathrm{app}}$ to be 44.4, 39.7, 29.4, 19.3, and 10.1 nm for kink spacings of 500, 250, 100, 50, and 25 nm, respectively. This is in excellent agreement with the numerical results by Yan and Marko [22].

We assumed thus far that the lifetime of the bound state of the kink-inducing proteins is large compared to the experimental timescales of the force-extension measurement [cf. Fig. 5(a)]. This assumption of longevity is valid if, for in-

stance, the affinities of the bound proteins and the corresponding kinetic barriers for loop unfolding are large as in the GalR and condensin cases. In the other limit of experimental time scales being much longer than the lifetime of the kink or loop, the numbers $N_i$ fluctuate and equilibrate [49] [cf. Fig. 5(b)]. In the ideal loop and kink gas regime, the mean loop and kink density of species $i$ becomes force dependent

$$\rho_i(F) = L^{-1}\langle N_i\rangle \sim \frac{1}{\lambda} e^{-\beta(\Delta G_i + (1/2)C(\alpha_i)\sqrt{AF})}, \tag{116}$$

where $\Delta G_i$ is the free energy of the kink and loop formation at $F=0$. The force-extension curve resulting from $\rho_i$ is a straightforward generalization of Eq. (112)

$$\frac{\langle \Delta x\rangle}{L} \approx 1 - k_B T(2\sqrt{AF})^{-1}\Big[1 + l_P \sum \rho_i(F) C(\alpha_i)\Big]. \tag{117}$$

In this case, the functional behavior of $\langle \Delta x(F)\rangle$ does not show the usual WLC form with a renormalized persistence length. For large enough forces, we have $l_P\rho_i(F) \to 0$ and one recovers as expected the bare DNA force extension response because there are no more kinks left to perturb the response [cf. Fig. 5(b)]. Interestingly, similar equations as (116) and (117) were independently derived by Popov and Tkachenko [21] using a variational method. Matching their notation $\lambda = l_0$, $\alpha = \pi - K$ and in the limit of $\alpha \ll 1$ (with their $K \approx \pi$), their Eq. (26) coincides with Eqs. (116) and (117). However for larger $\alpha \approx \pi$, our Eqs. (116) and (117) remain finite while the corresponding expression (26) of Ref. [21] diverges, which can be attributed to the limitations of the variational ansatz employed there.

## VI. CONCLUSION

We have calculated the partition function of DNA under tension featuring a sliding loop via a path integration in the semiclassical limit (i.e., on the level of a saddle-point approximation). This path integral can be mapped onto the QM harmonic oscillator with a time-dependent frequency. In this analogy, the time dependence reflects the shape of the DNA chain. As it turns out, the planar ground-state solutions (Euler elastica) are always just "simple" enough to allow the exact solution of the corresponding path integral. The special choice of the parametrization of the tangent vector to the DNA has made the application of the semiclassical approximation possible because the singular measure term (due to inextensibility constraint) has been found to be negligible in this case.

Within the semiclassical approximation, the equation of state of looped DNA under tension for very stiff polymers is valid for any value of the applied force. The force-extension relation has been found to be expressed in terms of Jacobi elliptic functions, and the force-extension curve provides two different scalings for weak and strong forces. For long DNA chains, the semiclassical approximation is valid only in the regime of strong stretching. In this force regime, we proved that the elastic response of DNA is (up to logarithmic corrections) indistinguishable from the response of a nonlooped WLC with the same contour length but a smaller persistence length. As we demonstrated, the entropic fluctuations of the system are only marginally affected by the DNA shape, i.e., the entropies of the overall straight and of the looped conformation are essentially the same. What changes considerably when going to the looped state is the enthalpic part. It is the latter contribution that causes the apparent renormalization of the chain stiffness. This remarkable effect suggests that the results of corresponding micromanipulation experiments have to be interpreted carefully, especially in the case when the contour length of the chain is on the order of its persistence length.

The looped DNA chain that we presented here should be considered as a paradigmatic model case. We believe that in the future this powerful approach will be applicable to a wide range of problems regarding semiflexible polymers. To stress this point, in this paper we have presented a few immediate generalizations: DNA that features a kink with a fixed angle as it might be induced by a protein and DNA carrying several defects (loops and/or kinks) along its contour. Having analytical expressions at hand allows one to directly extract microscopic information on DNA-protein complexes from micromanipulation experiments. We applied our theory to two complexes, the GalR-loop and the condensin complex and tested microscopic models with the help of our theory. For the GalR case, we were able to verify the antiparallel loop model [48]. For the condensin complex the experimental data are compatible with the loop-fastener model [46], but more systematic experiments in a whole range of stretching forces would be necessary to verify this model. We presently extend our formalism to many more cases, including a semiclassical formalism for the buckling of rigid chains [50], e.g., of microtubuli [51], or DNA tetrahedra [52].

## ACKNOWLEDGMENTS

The authors thank Vladimir Lobaskin, Nikhil Gunari, Andreas Janshoff, and Phil Nelson for discussion. I.M.K. was supported in part by NSF Grant Nos. DMR04-04674 and DMR04-25780.

## APPENDIX A: THE OUT-OF-PLANE DETERMINANT

In this appendix, we compute the out-of-plane determinant in the presence of a small magnetic field $D_\perp^\kappa(-L/2\lambda, L/2\lambda)$ associated to the following out-of-plane fluctuation operator [cf. Eq. (62)]:

$$\hat{\mathbf{T}}_\perp^\kappa = -\frac{\partial^2}{\partial t^2} + 6\,\mathrm{sn}^2\left(\frac{t}{\sqrt{m}}|m\right) - \left(\frac{4+m}{m}\right) + \frac{\kappa}{F}. \tag{A1}$$

In order to obtain a usual Lamé equation, we consider the transformation $t' \to \frac{t}{\sqrt{m}}$ so that $\hat{\mathbf{T}}_\perp$ can be written as

$$\hat{\mathbf{T}}_\perp^\kappa = \frac{1}{m}\left(-\frac{\partial^2}{\partial t'^2} + 6m\,\mathrm{sn}^2(t'|m) - (4+m) + 3k\right). \tag{A2}$$

Here, we introduce $3k/m = \kappa/F$ for later convenience. It can be shown [42] that the determinant is given by a particular

solution of the following generalized second-order Lamé differential equation:

$$\hat{\mathbf{T}}_{\perp}^{\kappa} y(t') = 0. \tag{A3}$$

Specifically, the solution satisfying the following boundary conditions:

$$y[-K(m)] = 0, \quad \text{and} \quad \left.\frac{dy}{dt'}\right|_{-K(m)} = \sqrt{m} \tag{A4}$$

gives the desired result via $D_{\perp}^{\kappa}(-\frac{L}{2\lambda}, \frac{L}{2\lambda}) = y[K(m)]$.

We now solve Eq. (A3) with a method suggested in Whittaker and Watson's book [53]. We first rewrite Eq. (A3) in the form

$$y'' - (6m\,\mathrm{sn}^2(t|m) - \varepsilon) y = 0, \tag{A5}$$

with $\varepsilon = 4 + m - 3k$, and introduce the periodic variable

$$z = \mathrm{cn}^2(t|m) \tag{A6}$$

in terms of which Eq. (A5) becomes

$$p(z)y'' + q(z)y' + r(z)y = 0, \tag{A7}$$

with $p(z) = -mz^3 + (2m-1)z^2 + (1-m)z$. Now consider two linear independent solutions $y_1(z)$ and $y_2(z)$ from which we build the function $M(z) = y_1(z)y_2(z)$. One can then prove that this function satisfies the following third-order differential equation:

$$2p(z)M'''(z) + 3p'(z)M''(z) + \{p''(z) + 2[\varepsilon + 6m(z-1)]\}M'(z) + 6mM(z) = 0, \tag{A8}$$

whose solution is a simple periodic function of the form $M(z) = z^2 + az + b$ with the coefficients

$$a = \frac{4 - 2m - \varepsilon}{3m} \quad \text{and} \quad b = \frac{(1 + m - \varepsilon)(4 + m - \varepsilon)}{9m^2}. \tag{A9}$$

Because the Wronskian $W$ of Eq. (A7) is given by $W = y_1\dot{y}_2 - y_2\dot{y}_1 = \frac{C}{\sqrt{z(1-z)(1-mz)}}$, we can deduce that the solutions of Eq. (A7) are necessarily of the form

$$y_{1,2}(z) = \sqrt{M(z)} \exp\left(\frac{\pm C}{2} \int \frac{dz}{\sqrt{p(z)M(z)}}\right), \tag{A10}$$

with

$$C = \frac{1}{9m^2}\{(4 + m - \varepsilon)(1 + m - \varepsilon)(1 + 4m - \varepsilon) \times [\varepsilon^2 - 4(1 + m)\varepsilon + 12m]\}^{1/2}. \tag{A11}$$

Introducing the transformation $z = 1 - \sin^2\phi$, the integral in Eq. (A10) can be rewritten

$$J = 2 \int \frac{d\phi}{\sqrt{1 - m\sin^2\phi} M(\sin^2\phi)}. \tag{A12}$$

With the help of the following fractional decomposition:

$$\frac{1}{M(\sin^2\phi)} = \frac{D_1}{1 - \frac{\sin^2\phi}{B_1}} + \frac{D_2}{1 - \frac{\sin^2\phi}{B_2}}, \tag{A13}$$

where the coefficients are given by

$$B_1 = \frac{2 + a - \sqrt{a^2 - 4ab}}{2}, \quad B_2 = \frac{2 + a + \sqrt{a^2 - 4ab}}{2} \tag{A14}$$

and

$$D_1 = \frac{2 + a - \sqrt{a^2 - 4ab}}{2(1 + a + b)\sqrt{a^2 - 4ab}}, \quad D_2 = \frac{2 + a + \sqrt{a^2 - 4ab}}{2(1 + a + b)\sqrt{a^2 - 4ab}}. \tag{A15}$$

Equation (A12) can be written in terms of the Jacobi elliptic function of the third kind $\Pi[n;\varphi\backslash m]$,

$$J(z) = 2D_1\Pi\left[\frac{1}{B_1}; \arcsin\sqrt{1-z}\backslash m\right] + 2D_2\Pi\left[\frac{1}{B_2}; \arcsin\sqrt{1-z}\backslash m\right], \tag{A16}$$

with

$$\Pi[n;\varphi\backslash m] = \int^{\varphi} \frac{d\phi}{(1 - n\sin^2\phi)(1 - m\sin^2\phi)^{1/2}}. \tag{A17}$$

Then, formally, the solution of Eq. (A5) can be written

$$y_{1,2}(t) = \sqrt{M(t)} \exp\left(\frac{\pm C}{2} J(t)\right). \tag{A18}$$

At this point, we mention that for $\kappa > 0$, $C$ is complex. Then, the solution satisfying the boundary conditions Eq. (A4) is given by the following linear combination of two solutions given in Eq. (A10):

$$y(t) = \frac{-\sqrt{m}\sqrt{M(-K)}}{|C|} \sqrt{M(t)} \sin\left(\frac{|C|}{2}\left[\frac{J(-K) - J(t)}{2}\right]\right). \tag{A19}$$

This solution is valid only the interval $-K[m] < t < 0$ because of relation Eq. (A6) between $z$ and $t$. Note that

$$J(-K[m]) = 2D_1\Pi\left[\frac{1}{B_1}, m\right] + 2D_2\Pi\left[\frac{1}{B_2}, m\right]. \tag{A20}$$

In order to compute the determinant, we need the solution $y(t)$ for $0 < t < K[m]$ that is also a linear combination of solution Eq. (A10)

$$y(t) = -\sqrt{m}\frac{\sqrt{M(K)}}{|C|} \sqrt{M(t)} \sin\left[\frac{|C|}{2}[J(t) + J(K[m])]\right]. \tag{A21}$$

Then for $t = K[m]$, we deduce the determinant $D_{\perp}^{\kappa} = y(K[m])$ so that

$$D_{\perp}^{\kappa} = -\sqrt{m}\frac{M(K[m])}{|C|}\sin[|C|J(K[m])]. \tag{A22}$$

This expression is valid for any value of $\kappa$ and could be used for the study of looped DNA in strong magnetic fields. Here, instead, we are interested in considering the limit of very small $\kappa$ (or, equivalently, $k$). For this we consider the expansion of the Jacobi elliptic function.

Expansion of $\Pi\left[\frac{1}{B_1}\backslash m\right]$:

From Eq. (A14), we deduce the expansion $B_1 \approx -\frac{1-m}{m^2}k + O(k^2)$. $B_1$ being negative, we find the following relation [40]:

$$\Pi\left[n=\frac{1}{B_1},m\right] = \frac{n(m-1)}{(1-n)(m-n)}\Pi[N,m] + \frac{m}{m-n}K[m], \tag{A23}$$

with $N=\frac{m-n}{1-n}$. As $m<N<1$, we have also $\Pi[N,m]=K[m] + \frac{\pi}{2}\delta_2[1-\Lambda_0(\varepsilon)]$, where $\Lambda_0(\varepsilon)$ is Heuman's Lambda function with

$$\varepsilon = \arcsin\sqrt{\frac{1-N}{(1-m)}} = \arcsin\sqrt{\frac{1}{1-n}} \approx \frac{1}{m}\sqrt{(1-m)k} \tag{A24}$$

and

$$\delta_2 = \sqrt{\frac{N}{(1-N)(N-m)}} = \sqrt{\frac{(m-n)(n-1)}{n(1-m)^2}} \approx \frac{m}{(1-m)\sqrt{(1-m)k}}. \tag{A25}$$

From the relation $\Lambda_0(\varepsilon)=\frac{2}{\pi}\{K[m]E[\varepsilon,1-m]-(K[m]-E[m])F[\varepsilon,1-m]\}$ and using the two expansions $E[\varepsilon,1-m]\approx\varepsilon$ and $F[\varepsilon,1-m]\approx\varepsilon$, we deduce

$$\Lambda_0(\varepsilon) \approx \frac{2}{\pi}\varepsilon E[m] \approx \frac{2E[m]}{\pi m}\sqrt{(1-m)k}. \tag{A26}$$

Now from Eqs. (A11) and (A15), we have the expansions

$$D_1 \approx -\frac{m^2}{(1-m)k} \quad \text{and} \quad |C| \approx \frac{1}{m}\sqrt{k(1-m)}, \tag{A27}$$

which allows one to write, finally,

$$2|C|D_1\Pi\left[\frac{1}{B_1},m\right] \approx 2\sqrt{\frac{(1-m)k}{m}}(E[m]-K[m]) - \pi. \tag{A28}$$

Expansion of $\Pi\left[\frac{1}{B_2}\backslash m\right]$:

From Eq. (A14), we deduce the expansion $B_2 \approx 1+\frac{k}{m^2}$. Since $B_2>1$ and $m<\frac{1}{B_2}<1$, we can use the relation

$$\Pi\left[n=\frac{1}{B_2},m\right] = K[m] + \frac{\pi}{2}\delta_2[1-\Lambda_0(\varepsilon)], \tag{A29}$$

where

$$\varepsilon = \arcsin\sqrt{\frac{1-n}{(1-m)}} \approx \frac{1}{m}\sqrt{\frac{k}{(1-m)}} \tag{A30}$$

and

$$\delta_2 = \sqrt{\frac{n}{(1-n)(n-m)}} \approx \frac{m}{\sqrt{(1-m)k}} \tag{A31}$$

so that, finally,

$$\Lambda_0(\varepsilon) \approx \frac{2}{\pi}\varepsilon E[m] \approx \frac{2E[m]}{\pi m}\sqrt{\frac{k}{(1-m)}}. \tag{A32}$$

As $D_2 \approx -m^2 + O(k)$, we find

$$2|C|D_2\Pi\left[\frac{1}{B_2}\backslash m\right] \approx \frac{2}{m}\sqrt{\frac{k}{(1-m)}}(E[m]-(1-m)K[m]) - \pi. \tag{A33}$$

Collecting the two expressions (A28) and (A33), we deduce that

$$\sin[|C|J(K[m])] \approx \frac{2}{m}\sqrt{\frac{k}{(1-m)}}((2-m)E[m] - 2(1-m)K[m] - 2\pi). \tag{A34}$$

With this result in hand and with the expansion $M(2K[m]) \approx \frac{k}{m^2}$, we deduce that the determinant (A22) becomes in the small $k$ limit

$$D_{\perp}^{\kappa} \approx \frac{2k\sqrt{m}}{m^2(1-m)}(2(1-m)K[m]-(2-m)E[m]), \tag{A35}$$

which writes in terms of $\kappa$

$$D_{\perp}^{\kappa} \approx \frac{2\kappa}{3F}\frac{1}{\sqrt{m}(1-m)}(2(1-m)K[m]-(2-m)E[m]). \tag{A36}$$

## APPENDIX B: COMPUTATION OF THE PERPENDICULARLY CONSTRAINED PARTITION FUNCTION IN THE LIMIT OF INFINITE LONG CHAIN

Here we evaluate the path integral given by Eq. (97). It is equivalent to a special realization of the path integral of a QM harmonic oscillator with a time-dependent frequency $\omega(\tau)$ and a driving force $j(\tau)$

$$I[\omega,j] = \int_{(x_0,\tau_0)}^{(x_1,\tau_1)} \mathcal{D}[x]e^{(i/\hbar)S[j,x]} = \int_{(x_0,\tau_0)}^{(x_1,\tau_1)} \mathcal{D}[x]e^{(i/\hbar)\{\int_{\tau_0}^{\tau_1}(m/2)[\dot{x}^2(\tau)-\omega^2(\tau)x^2(\tau)]d\tau+\int_{\tau_0}^{\tau_1}j(\tau)x(\tau)d\tau\}}. \tag{B1}$$

The latter can be computed exactly (cf. Ref. [23], Chap. 4)

$$I[\omega,j]=\sqrt{\frac{m}{2\pi i\hbar\, D(\tau_1,\tau_0)}}e^{(i/\hbar)S[j,x_{cl}]}. \tag{B2}$$

The first factor on the right-hand side of Eq. (B2) represents the fluctuation contribution. Here, $D(\tau_1,\tau_0)$ is the functional determinant of the ($j$-independent) operator $\hat{\mathbf{T}}=d^2/d\tau^2+\omega^2(\tau)$ normalized by the free-particle operator $d^2/d\tau^2$

$$\frac{D(\tau_1,\tau_0)}{\tau_1-\tau_0}=\det\left(\frac{d^2/d\tau^2+\omega^2(\tau)}{d^2/d\tau^2}\right). \tag{B3}$$

The second term in Eq. (B2) involves the classical action $S[j,x_{cl}]$, where the $j$-dependent classical path $x_{cl}(\tau)$ is the solution of the corresponding Euler-Lagrange equation

$$m\ddot{x}_{cl}(\tau)+m\omega^2(\tau)x_{cl}(\tau)=j(\tau). \tag{B4}$$

with boundary conditions $x_{cl}(\tau_{0/1})=x_{0/1}$. Using Eq. (B4), the classical action can be rewritten as

$$S[j,x_{cl}]=\frac{m}{2}xcl(\tau)\dot{x}_{cl}(\tau)|_{\tau_0}^{\tau_1}+\frac{1}{2}\int_{\tau_0}^{\tau_1}j(\tau)x_{cl}(\tau)d\tau. \tag{B5}$$

Now in our concrete case we have to evaluate

$$\hat{Q}_\perp(p)=\int_{(0,t_0)}^{(0,t_1)}\mathcal{D}[\delta\vartheta]e^{-(\beta\sqrt{AF}/2)\int_{t_0}^{t_1}\delta\vartheta\hat{\mathbf{T}}_\perp^\kappa\delta\vartheta dt+\int_{t_0}^{t_1}j(t)\delta\vartheta dt}, \tag{B6}$$

with (asymptotic) boundary conditions at $t_{1/0}=\pm\frac{L}{2\lambda}\to\pm\infty$. The operator $\hat{\mathbf{T}}_\perp^\kappa$ is again given by

$$\hat{\mathbf{T}}_\perp^\kappa=\left(-\frac{\partial^2}{\partial t^2}-\frac{N(N+1)}{\cosh^2(t)}+c^2\right), \tag{B7}$$

with $c=\sqrt{1+\frac{\kappa}{F}}$ and $N=2$. The source term is given by $j(t)=-i\frac{p}{2t_c}[H(t+t_c)-H(t-t_c)]$. In our case, the integral (B2) (after "Wick rotation" $\tau\to-it$ and the replacement $1/\hbar\to\beta$, $m\to\sqrt{AF}$, $\omega^2(t)\to[1-6/\cosh^2(t)+\kappa/F]$, etc.) has the following form:

$$\hat{Q}_\perp(p)=\sqrt{\frac{\beta\sqrt{AF}}{2\pi D(t_1,t_0)}}e^{-\beta S[j,x_{cl}]}, \tag{B8}$$

with the classical action given by the following expression

$$\beta S[j,\delta\vartheta_{cl}]=\frac{\beta\sqrt{AF}}{2}\vartheta_{cl}(t)\dot{\vartheta}_{cl}(t)|_{-\infty}^{\infty}-\frac{1}{2}\int_{-\infty}^{\infty}j(\tau)\vartheta_{cl}(\tau)d\tau$$

$$=\frac{p^2}{2\beta\sqrt{AF}}\int_{-t_c}^{t_c}\int_{-t_c}^{t_c}G(t,t')dtdt'. \tag{B9}$$

We first compute the fluctuation determinant $D(-\frac{L}{2\lambda},\frac{L}{2\lambda})$ via the Gelfand-Yaglom method. It states that $D(-\frac{L}{2\lambda},\frac{L}{2\lambda})=f(t)|_{t=L/2\lambda}$, where $f(t)$ is the solution to $\hat{\mathbf{T}}_\perp^\kappa f(t)=0$ with initial values $f(-\frac{L}{2\lambda})=0$ and $\dot{f}(-\frac{L}{2\lambda})=1$. The solution can be written in terms of the two linearly independent solutions (cf. [54])

$$f_\pm(x)=\cosh^{N+1}(t)\left(\frac{1}{\cosh t}\frac{d}{dt}\right)^{N+1}e^{\pm ct}. \tag{B10}$$

For $N=2$, the two independent solutions are

$$f_1(t)=e^{ct}[(c-2\tanh t)(c-\tanh t)-\cosh^{-2}(t)]$$

$$f_2(t)=e^{-ct}[(c+2\tanh t)(c+\tanh t)-\cosh^{-2}(t)], \tag{B11}$$

and the general solution is given by $f(t)=C_1f(t)_1+C_2f(t)_2$. The Gelfand-Yaglom initial conditions in the limit $\frac{L}{2\lambda}\gg1$ [where we may safely set $\tanh(\pm\frac{L}{2\lambda})\approx\pm1$, $\cosh^{-2}(\frac{L}{2\lambda})\approx0$] determine the coefficients $C_1$ and $C_2$

$$C_1=\frac{1}{2c(c+2)(c+1)}e^{c(L/2\lambda)},$$

$$C_2=-\frac{1}{2c(c-2)(c-1)}e^{-c(L/2\lambda)}.$$

Evaluating $f(t)$ at the right boundary $t=\frac{L}{2\lambda}$, we obtain for $L/2\lambda\gg1$

$$D_\perp^\kappa\left(-\frac{L}{2\lambda},\frac{L}{2\lambda}\right)\approx\frac{(c-2)(c-1)}{2c(c+2)(c+1)}e^{c(L/\lambda)}. \tag{B12}$$

Note that unlike for the in-plane operator $Q_\parallel$ case (where a close to zero eigenmode appears and creates artifacts), here we need not to renormalize $D_\perp^\kappa(-\frac{L}{2\lambda},\frac{L}{2\lambda})$ and $Q_\perp^\kappa$ as long as the value of $c>2$.

To compute the classical action equation (B9), consider the Euler-Lagrange equation, which reads

$$\beta\sqrt{AF}\hat{\mathbf{T}}_\perp^\kappa\delta\vartheta_{cl}(t)=j(t), \tag{B13}$$

with the boundary conditions $\delta\vartheta_{cl}(\pm\infty)=0$. To solve this inhomogeneous differential equation, we construct the Green's function [55] $G(t,t')$ that is the solution to

$$\hat{\mathbf{T}}_\perp^\kappa G(t,t')=\delta(t-t'), \tag{B14}$$

with $G(t,t')=G(t',t)$ and proper boundary conditions $G(\pm\infty,t')=0$. The latter gives the solution to Eq. (B13) via the simple convolution

$$\delta\vartheta_{cl}(t)=(\beta\sqrt{AF})^{-1}\int_{-\infty}^{\infty}G(t,t')j(t')dt. \tag{B15}$$

For our Dirichlet boundary conditions the Green's function generally writes [55]

$$G(t,t')=-\frac{H(t'-t)f_2(t')f_1(t)+H(t-t')f_1(t')f_2(t)}{W}, \tag{B16}$$

with $f_1$ two $f_2$ being two (arbitrary) linearly independent solutions to the homogeneous equation $\hat{\mathbf{T}}_\perp^\kappa f=0$ satisfying the (one sided) boundary conditions $f_1(-\infty)=0$ and $f_2(\infty)=0$, respectively. The constant $W$ is the Wronski determinant of the two solutions, i.e.,

$$W = f_1(t)\dot{f}_2(t) - \dot{f}_1(t)f_2(t) = \text{const}. \tag{B17}$$

We already know the two solutions [cf. Eq. (B11)]. Their Wronskian (B17) is given after short computation by $W = -2c(c^2-2)(c^2-1)$. Inserting that and Eq. (B11) into Eq. (B16) gives a lengthy expression for $G(t,t')$. Fortunately, there is no need for writing out explicitly neither $G(t,t')$ nor $\delta\vartheta_{cl}(t)$ as we are only interested in $S[j,x_{cl}]$ from Eq. (B5) (with $x_{cl}=\delta\vartheta_{cl}$). Using Eq. (B15) together with the boundary condition $\delta\vartheta_{cl}(\pm\infty)=0$ leads to

$$\beta S[j,\delta\vartheta_{cl}] = \frac{p^2}{4\beta t_c^2\sqrt{AF}}\int_{-t_c}^{t_c}\int_{-t_c}^{t_c} G(t,t')dtdt'. \tag{B18}$$

Inserting the Green's function [Eq. (B16)] and exploiting $f_2(t)=f_1(-t)$, we find

$$\begin{aligned}\beta S[j,\delta\vartheta_{cl}] &= \frac{(\beta\sqrt{AF})^{-1}p^2}{4t_c^2c(c^2-2)(c^2-1)}\int_{-t_c}^{t_c} f_1(t') \\ &\quad\times\left[\int_{t'}^{t_c} f_1(-t)dt\right]dt' \\ &= \frac{(\beta\sqrt{AF})^{-1}p^2}{4t_c^2c(c^2-2)(c^2-1)}I(c,t_c).\end{aligned} \tag{B19}$$

The involved double integral $I(c,t_c)$ depends on the variable $c=\sqrt{1+\frac{\kappa}{F}}$ and the numerical constant $t_c$ in a complicated manner. But here we only need the case $\kappa\to 0$ (i.e., $c\to 1$). The expansion of the integrand around $c=1$ (to lowest order) followed by the double integration gives [up to terms on the order of $(c-1)^2$]

$$\begin{aligned}I(c,t_c) &= -6(c-1)\left(2t_c + 3\frac{t_c}{\cosh^2 t_c} - 5\tanh t_c\right) \\ &= \frac{3}{2}t_c(3t_c^2-10)(c-1) \approx 2.88(c-1).\end{aligned}$$

Here we made use of the definition of $t_c$ [Eq. (101)]. The limit $c\to 1$ (i.e., $\kappa\to 0$) can now be performed safely in Eq. (B19) and the action $S[j,\delta\vartheta_{cl}]$ writes

$$\lim_{\kappa\to 0}\beta S[j,\delta\vartheta_{cl}] = -\frac{3}{32}\frac{(3t_c^2-10)}{\beta t_c\sqrt{AF}}p^2 \approx -\frac{0.05}{\beta\sqrt{AF}}p^2. \tag{B20}$$

This leads finally to

$$\begin{aligned}\hat{Q}_\perp(p) &= \sqrt{\frac{\beta\sqrt{AF}}{2\pi D(t_1,t_0)}}e^{-\beta S[j,x_{cl}]} \\ &= \sqrt{\frac{l_P}{\lambda}\frac{c(c+2)(c+1)}{\pi(c-2)(c-1)}}e^{-c(L/2\lambda)}e^{(3/32)(\lambda/l_P t_c)(3t_c^2-10)p^2}.\end{aligned} \tag{B21}$$


[1] B. Alberts, *Molecular Biology of the Cell* (Garland, New York, 1989).

[2] T. R. Strick, M. N. Dessinger, G. Charvin, N. H. Dekker, J. F. Allemand, D. Bensimon, and V. Croquette, Rep. Prog. Phys. **66**, 1 (2003).

[3] S. B. Smith, L. Finzi, and C. Bustamante, Science **258**, 1122 (1992).

[4] T. R. Strick, J. F. Allemand, D. Bensimon, A. Bensimon, and V. Croquette, Science **271**, 1835 (1996).

[5] S. B. Smith, Y. Cui, and C. Bustamante, Science **271**, 795 (1996).

[6] M. D. Wang, Biophys. J. **72**, 1335 (1997).

[7] P. Cluzel, A. Lebrun, C. Heller, R. Lavery, J. L. Viovy, D. Chatenay, and F. Caron, Science **271**, 792 (1996).

[8] T. T. Perkins, D. E. Smith, R. G. Larson, and S. Chu, Science **268**, 83 (1995).

[9] R. Rief, M. Gautel, F. Osterhelt, J. M. Fernandez, and H. E. Gaub, Science **276**, 1109 (1997).

[10] C. Bustamante, Z. Bryant, and S. B. Smith, Nature (London) **421**, 423 (2003).

[11] Frenkel-Bresler theory is reviewed in L. D. Landau and E. M. Lifshitz, *Statistical Mechanics* (Pergamon Press, Oxford, 1996); O. Kratky and G. Porod, Recl. Trav. Chim. Pays-Bas **68**, 1106 (1949); M. Fixman and J. Kovac, J. Chem. Phys. **58**, 1564 (1973); J. Kovac and C. C. Crabb, Macromolecules **15**, 1112 (1982).

[12] C. Bustamante, J. F. Marko, E. D. Siggia, and S. Smith, Science **265**, 1599 (1994); A. Vologodskii, Macromolecules **27**, 5623 (1994); J. F. Marko and E. D. Siggia, *ibid.* **28**, 8759 (1995); T. Odijk, *ibid.* **28**, 7016 (1995); C. Bouchiat *et al.*, Biophys. J. **76**, 409 (1999).

[13] S. Sankararaman and J. F. Marko, Phys. Rev. E **71**, 021911 (2005).

[14] C. G. Baumann, V. A. Bloomfield, S. B. Smith, C. Bustamante, M. D. Wang, and S. M. Block, Biophys. J. **78**, 1965 (2000).

[15] Y. Murayama, Y. Sakamaki, and M. Sano, Phys. Rev. Lett. **90**, 018102 (2003).

[16] H. Noguchi, S. Saito, S. Kidoki, and K. Yoshikawa, Chem. Phys. Lett. **261**, 527 (1996); B. Schnurr, F. Gittes, and F. C. MacKintosh, Phys. Rev. E **65**, 061904 (2002).

[17] T. R. Strick, J. F. Allemand, D. Bensimon, and V. Croquette, Biophys. J. **74**, 2016 (1998).

[18] J. D. Moroz and P. Nelson, Proc. Natl. Acad. Sci. U.S.A. **94**, 14418 (1997); Macromolecules **31**, 6333 (1998); C. Bouchiat and M. Mezard, Phys. Rev. Lett. **80**, 1556 (1998); Eur. Phys. J. E **2**, 377 (2000).

[19] R. Metzler, Y. Kantor, and M. Kardar, Phys. Rev. E **66**, 022102 (2002).

[20] R. Bruinsma and J. Rudnick, Biophys. J. **76**, 1725 (1999).

[21] Y. O. Popov and A. V. Tkachenko, Phys. Rev. E **71**051905 (2005).

[22] J. Yan and J. F. Marko, Phys. Rev. E **68**, 011905 (2003).

[23] H. Kleinert, *Path Integrals* (World Scientific, Singapore, 2002).

[24] J. Zinn-Justin, *Quantum Field Theory and Critical Phenomena* (Clarendon Press, Oxford, 1993).
[25] I. M. Kulić, H. Mohrbach, V. Lobaskin, R. Thaokar, and H. Schiessel, Phys. Rev. E **72**, 041905 (2005).
[26] G. Lia, D. Bensimon, V. Croquette, J.-F. Allemand, D. Dunlap, D. E. A. Lewis, S. Adhya, and L. Finzi, Proc. Natl. Acad. Sci. U.S.A. **100**, 11373 (2003).
[27] I. M. Kulić and H. Schiessel, Phys. Rev. Lett. **92**, 228101 (2004).
[28] B. Maier and J. O. Rädler, Phys. Rev. Lett. **82**, 1911 (1999).
[29] G. Maret, M. V. Schickfus, A. Mayer, and K. Dransfeld, Phys. Rev. Lett. **35**, 397 (1975).
[30] L. D. Landau and E. M. Lifshitz, *Theory of Elasticity* (Pergamon Press, London, 1996).
[31] P. J. Hagerman, Annu. Rev. Biophys. Biophys. Chem. **17**, 265 (1988).
[32] C. J. Benham, Proc. Natl. Acad. Sci. U.S.A. **74**, 2397 (1977); C. J. Benham, Biopolymers **18**, 609 (1979); M. Le Bret, *ibid.* **18**, 1709 (1979); M. Le Bret, *ibid.* **23**, 1835 (1984).
[33] G. Kirchhoff, J. Reine Angew. Math. **56**, 285 (1859).
[34] M. Nizette and A. Goriely, J. Math. Phys. **40**, 2830 (1999).
[35] T. Odijk, J. Chem. Phys. **105**, 1270 (1996).
[36] T. Odijk, Macromolecules **19**, 2313 (1986).
[37] P. G. de Gennes, *Scaling Concepts in Polymer Physics* (Cornell University Press, Ithaca, 1979).
[38] The term homoclinic stems from the Kirchhoff analogy between the loop that we consider here and the homoclinic orbit of a (mathematical) pendulum that obtained just enough energy to make one full $2\pi$ rotation in an infinite time interval.
[39] A. S. Davydov, *Solitons in Molecular Systems* (Kluwer, Dordrecht, 1985).
[40] M. Abramowitz and I. Stegun, *Handbook of Mathematical Functions* (Dover, New York, 1972).
[41] F. M. Arscott, *Periodic Differential Equations* (Pergamon Press, London, 1964).
[42] I. M. Gelfand and A. M. Yaglom, J. Math. Phys. **1**, 48 (1960).
[43] D. R. M. Williams, J. Phys. A **24**, 4427 (1991).
[44] The diamagnetic anisotropy per length $\chi_a/h$ of a single base-pair is around $3\times10^{-6}pN/T^2$ [29], i.e., for even very large magnetic fields of say $H=15T$, we have $\kappa\approx7\times10^{-4}pN$. Thus, for DNA this effect is rather small.
[45] J. S. Langer, Ann. Phys. **41**, 108 (1967).
[46] K. A. Hagstrom and B. J. Meyer, Nat. Rev. Genet. **4**, 521 (2003).
[47] T. R. Strick, T. Kawaguchi, and T. Hirano, Curr. Biol. **14**, 874 (2004).
[48] M. Geanacopoulos *et al.*, Nat. Struct. Biol. **8**, 432 (2001).
[49] On timescales slightly longer than (but still comparable to) the loop life time one observes jumps in the force-extension curve, i.e., the so-called "stick-slip" behavior in combination with an abruptly changing $l_P^{app}$ as observed in stretching experiments on DNA condensed with multivalent counterions [14].
[50] M. Emanuel, H. Mohrbach, M. Sayar, H. Schiessel, and I. M. Kulić (unpublished).
[51] M. E. Janson and M. Dogterom, Phys. Rev. Lett. **92**, 248101 (2004).
[52] R. P. Goodman *et al.*, Science **310**, 1661 (2005).
[53] E. T. Whittaker and G. N. Watson, *A Course of Modern Analysis* (Cambridge Mathematical Library, Cambridge, England, 1996).
[54] E. Kamke, *Differential Equations, Methods and Solutions* (Akademie-Verlag, Leipzig, 1959).
[55] G. Barton, *Elements of Green's Functions and Propagation* (Oxford Science Publications, London, 1989).